The minimal cell-cycle control system in *Marchantia* as a framework for understanding plant cell proliferation

Facundo Romani[1,†], Ignacy Bonter[1], Marius Rebmann[1], Go Takahashi[2], Fernando Guzman-Chavez[3], Francesco De Batté[1], Yuki Hirakawa[2], Jim Haseloff[1,†]

[1] Department of Plant Sciences, University of Cambridge, Cambridge, CB2 3EA, UK.

[2] Graduate School of Integrated Sciences for Life, Hiroshima University, Higashi Hiroshima, Hiroshima 739-8526, Japan

[3] Faculty of Chemistry, Food and Biotechnology Department, Universidad Nacional Autónoma de México UNAM, Ciudad Universitaria, Mexico City, 04510, México.

[†] Author for correspondence: fr391@cam.ac.uk, jh295@cam.ac.uk

ABSTRACT

The regulation of cell division is broadly conserved across eukaryotes, governed by cyclins and cyclin-dependent kinases (CDKs) to coordinate progression through the cell cycle. Plants have evolved a complex set of cell-cycle genes with unique features. The high number of cyclin-CDK pairs in flowering plants complicates functional studies due to redundancy and diversification. It is critical to study simple systems in other plant lineages to better understand the functional integration of the cell-cycle control machinery and its evolution across land plants.

Through a comprehensive phylogenetic analysis, we show that non-seed plants possess a simple repertoire of cyclin and CDK proteins, suggesting that the observed complexity in seed plants is a derived trait. The liverwort *Marchantia polymorpha* possess a streamlined set of core cell cycle genes with minimal redundancy during vegetative development. Using single-cell RNA-seq and fluorescent reporters, we found a precise, phase-specific pattern of expression for cell cycle genes. We

demonstrated *in vivo* that only three cyclins are active, one at a given phase, without redundancy. Functional analyses revealed that Mp*CYCD;1* promotes cell cycle re-entry and disrupts differentiation, while overexpression of Mp*CYCA* or Mp*CYCB;1* arrests the cell cycle, consistent with their respective roles at G1, S, and G2/M progression.

Our findings highlight the functional conservation of mechanisms for cell-cycle control across eukaryotes and provide insights into its ancestral state, revealing a minimal set of functional components required for multicellular development. This study advances our understanding of fundamental aspects of cell-cycle regulation and opens new possibilities for engineering plant growth.

Keywords: cell cycle, evolution of development, Marchantia, cyclin-dependent kinases, cyclins.

41 **INTRODUCTION**

42 Eukaryotic organisms have evolved sophisticated mechanisms to control cell
43 proliferation. While cell-cycle control shares common features across eukaryotes, with
44 a conserved set of molecular mechanisms, different lineages such as plants, animals,
45 and fungi adapted it to different multicellular body plans and developmental
46 programmes. Understanding these regulatory networks is a central question for
47 developmental biology and the evolution of development. This knowledge could be
48 instrumental for rational engineering of development and neoorganogenesis in crop
49 plants and promote advances in agricultural biotechnology (Brophy et al., 2018).

50 The eukaryotic mitotic cell cycle progress through G1 (gap 1), S (synthesis), and G2
51 (gap 2) phases to in mitosis (M) (Mironov et al., 1999; Krylov et al., 2003). The
52 transition between phases is governed by a relay of cyclins that activate cyclin-
53 dependent kinases (CDKs) to ensure the proper coordination of replication and
54 chromosome segregation. Group I cyclins are unequivocally associated with cell cycle
55 regulation (Martinez-Alonso and Malumbres, 2020), following an archetypical
56 sequence: D-type cyclins regulate the G1/S transition, A-type cyclins are linked to the
57 S-phase, and B-type cyclins with the G2/M transition (Inze and De Veylder, 2006;
58 Komaki and Sugimoto, 2012). The interaction of cyclins with their CDK partners
59 phosphorylate the retinoblastoma (RB) protein and trigger the transduction of signals
60 necessary for the division of the cells. The regulation of these networks is not only
61 crucial for controlling the rate of cell division but also for maintaining the appropriate
62 balance between proliferation and differentiation, and essential for functional integrity,
63 proper organ formation and integration of environmental responses (Inze and De
64 Veylder, 2006).

65 While the canonical organization of phase specific cyclins/CDKs is well portrayed in
66 the literature and textbooks, most model organisms have different sets of genes that
67 further complicate and specialize this system. For example, animals have E-type
68 cyclins, another G1 specific cyclin that overlaps with D-type, and yeast do not have a
69 true A-type cyclin ortholog. This question is of special importance in plants. The first
70 plant cell cycle components were identified in *Arabidopsis thaliana* as homologs of
71 yeast and animal regulators (Gutierrez, 2009). Plants also exhibit unique cell cycle

features, such as a plant-specific CDKB expressed during G2/M (Gutierrez, 2009). The high complexity of cyclin and CDK regulation, especially in flowering plants, has made it challenging to disentangle their precise functional roles in the progression of the cell cycle in plants (Gutierrez, 2022) and has hindered our ability to understand many fundamental aspects of the cell cycle regulation and evolution.

The Arabidopsis genome displays a large repertoire of cell cycle genes, including 31 Group I cyclins. Among the 10 D-type cyclins, some peak at G1, others at S, and others at G2/M, and only *CYCD3;3* and *CYCD5;1* follow the canonical expression pattern (Menges et al., 2005; Menges et al., 2006). Similarly, expression of the A-type *CYCA3* subfamily peaks at S, while *CYCA1* and *CYCA2* peak at G2/M (Menges et al., 2005). Only B-type cyclins and CDKB genes are consistently expressed at G2/M (Menges et al., 2005). This diversity of expression patterns could be a consequence of gene redundancy and cell cycle specialization. The question of how this system may have worked in early land plant ancestors is yet unresolved.

To understand the plant cell cycle regulation, it is crucial to employ diverse model species. Research in green algae like *Chlamydomonas reinhardtii* has provided critical insights into the fundamental architecture of the cell cycle (Cross and Umen, 2015; Tulin and Cross, 2015; Atkins and Cross, 2018; Breker et al., 2018; Cross, 2020), including conservation of the regulation of the anaphase-promoting complex by the plant specific CYCB/CDKB complex (Pecani et al., 2022). However, *Chlamydomonas* exhibit an uncommon multiple-fission cell cycle, that consists of a long G1 phase followed by successive rounds of S phases and M (Cross and Umen, 2015), making it hard to compare with other plant species. Non-vascular plants offer a promising opportunity to study the cell cycle in early divergent plants, with different cellular body plans. The moss *Physcomitrium patens* has revealed both conserved and unique aspects of plant cell cycle regulation (Schween et al., 2008; Ishikawa et al., 2011; Peramuna et al., 2023). However, the large repertoire of cyclins and CDKs in *Physcomitrium* creates challenges for understanding due to functional redundancy.

The model liverwort *Marchantia polymorpha*, features a reduced set of cell-cycle regulators (Bowman et al., 2017). Its simplicity positions Marchantia as a key organism to study the evolution of developmental and systems biology (Bowman et

103 al., 2022; Romani et al., 2024) and could be instrumental to understand the evolution
104 of the cell-cycle control system across land plants without the confounding effects of
105 gene redundancy and sub-functionalization. However, functional studies in this
106 species are lacking.

107 In this work, we made a comprehensive phylogenetic analysis of cell cycle genes
108 across plants and other eukaryotes and observed that Marchantia retains a minimal
109 set of regulators. Expression profiles and functional analyses allowed us to elucidate
110 the organization of the core cell cycle regulation genes that operate in Marchantia and
111 compare this system with its counterparts in other eukaryotes. Functional analyses of
112 cyclin genes in the Marchantia vegetative gametophyte revealed that Mp*CYCD;1* is a
113 rate-limiting factor for cell proliferation, promoting dedifferentiation, while Mp*CYCB;1*
114 and Mp*CYCA* causes cell cycle arrest. Overall, these results provide a model of the
115 streamlined cell-cycle control system in Marchantia and will be useful to navigate study
116 of the cell cycle and future approaches to engineering plant growth and development.

117

118 **RESULTS**

119 **Phylogenetic analysis of core cell cycle genes**

120 To investigate the core regulation of cell cycle regulation in land plants, we conducted
121 a phylogenetic analysis of cell cycle genes in a broad range of 27 eukaryotic species,
122 including yeast, animals, brown and red algae, charophytes, bryophytes, lycophytes,
123 ferns, and flowering plants (Figure 1). We focused on gene families that have been
124 described as fundamental components of the cell-cycle control machinery, including:
125 Group I cyclins, CDKs, CYCLIN-DEPENDENT KINASES REGULATORY SUBUNIT
126 (CKS), RETINOBLASTOMA-RELATED (RBR) proteins, and the associated
127 transcription factors (TFs) from the E2F, DP, DEL, and 3R-MYB gene families.

128 A-, B-, and D-type cyclins are well conserved across eukaryotes, except fungi, which
129 only display two classes of cyclins (Ma et al., 2013) corresponding to the B- and D-
130 type (Figure 1a,c). E-type cyclins are specific to animals, with potential presence in
131 other green algal lineages but absent in land plants (Figure 1a-b). SOLO DANCERS
132 (SDS) cyclins are a group of plant-specific cyclins associated with meiosis (Azumi et

133 al., 2002) that likely originated in charophytic algae but those genes were
134 subsequently lost in some non-seed plants (Figure 1c). Interestingly, there is a gene
135 duplication of the D-type cyclins that appear to have given rise to a new clade of
136 bryophyte-specific cyclins that we named CYCD' (Figure 1a,c).

137 CDKAs and CDKBs are the main partners that interact with cyclins to help govern cell-
138 cycle progression in plants. CDKA, homologous to yeast CDC28, is conserved across
139 eukaryotes with the hallmark PSTAIRE motif (Figure 1b-c, Suppl. Figure 2). The G2/M
140 specific CDKB is ubiquitously present in all green plants (Figure 1b-c). In non-flowering
141 plants, they are associated with the PSTALRE motif (Figure 1b) that is well conserved
142 across the family, as opposed to the P(P/S)T(A/T)LRE in flowering plants (Joubes et
143 al., 2000). The only case in which this motif is found in CDKBs outside the green algae
144 are the brown algae, *Ectocarpus siliculosus*, which contain two divergent CDKB-like
145 CDKs with the PSTALRE motif (Figure 1b).

146 Other CDKs can act as activators within the cell cycle phosphorylation cascade
147 (Joubes et al., 2000). CDKC (homologous to yeast CTK), CDKD (KIN28), CDKE
148 (CAK1/SSN3), and CDKG are conserved across eukaryotes, with some lineage-
149 specific losses (Figure 1b-c). Notably, the CDKC subfamily has expanded in plants,
150 forming a distinct streptophyte-specific CDK-like clade, whose function is largely
151 unknown. (Joubes et al., 2000). Among the remaining clades, CDKF is found in all
152 streptophytes, and the PHO85 clade, which belong to the CDKA/CDC28 super-family,
153 is conserved in yeast and animals but not found in most other eukaryotes (Liu and
154 Kipreos, 2000). Divergent CDKAB members form a paraphyletic group in scattered
155 species, lacking conserved motifs. CKS genes are broadly conserved, except in the
156 charophyte algae *Mesostigma viridae* (Figure 1c).

157 Downstream of CDK signalling, the RBR pathway is essential for cell cycle progression
158 and is also highly conserved, with a single RBR homologue in most species. There
159 are three clades of RBR-related TFs that form part of the DREAM complex during the
160 G1/S transition (E2F, DP, and DEL). The three clades share a common evolutionary
161 origin (Rauber et al., 2016). E2F and DP TFs form highly conserved heterodimers to
162 regulate the onset of DNA replication. Both protein families are present in animals and
163 plants, suggesting an early origin of the interaction (Figure 1c). In contrast, DEL

164 proteins, which are present in both brown algae and plants, have been lost in several
165 plant lineages.

166 The 3R-MYB TFs (or c-Myb in animals), which regulate the G2/M transition (Ito et al.,
167 2001), show a common origin before the divergence of plants and animals (Kobayashi
168 et al., 2015; Feng et al., 2017), with some lineages losing one of the MYB domains.
169 All plant species contain at least one 3R-MYB gene, except for the algae species
170 *Chlamydomonas* and *Penium margaritaceum* (Figure 1c).

171 In charophytes, including the algal sister lineage of land plants (Feng et al., 2024), and
172 bryophytes, most cell-cycle genes exist as single copies, suggesting that the common
173 ancestor of land plants possessed a minimal set of these core components. This set
174 has expanded considerably in some lineages, particularly in flowering plants,
175 consistent with the pattern of whole-genome duplications. Remarkably, the liverwort
176 *Marchantia polymorpha* retains a simplified set of cell cycle regulators, with highly
177 reduced redundancy compared to vascular plants. It has single copies of most cell
178 cycle regulators, except for CYCD (Mp*CYCD;1* and Mp*CYCD;2*) CYCB (Mp*CYCB;1*
179 and Mp*CYCB;2*), and CDKC (MpCDKC;1 and MpCDKC;2), and a considerable
180 repertoire of TFs, including 3 DP (Mp*DP1*, Mp*DP2*, and Mp*DP3*), 2 DEL (Mp*DEL1* and
181 Mp*DEL2*), and 9 3R-MYBs (Mp*3R-MYB1* to Mp*3R-MYB9*).

182

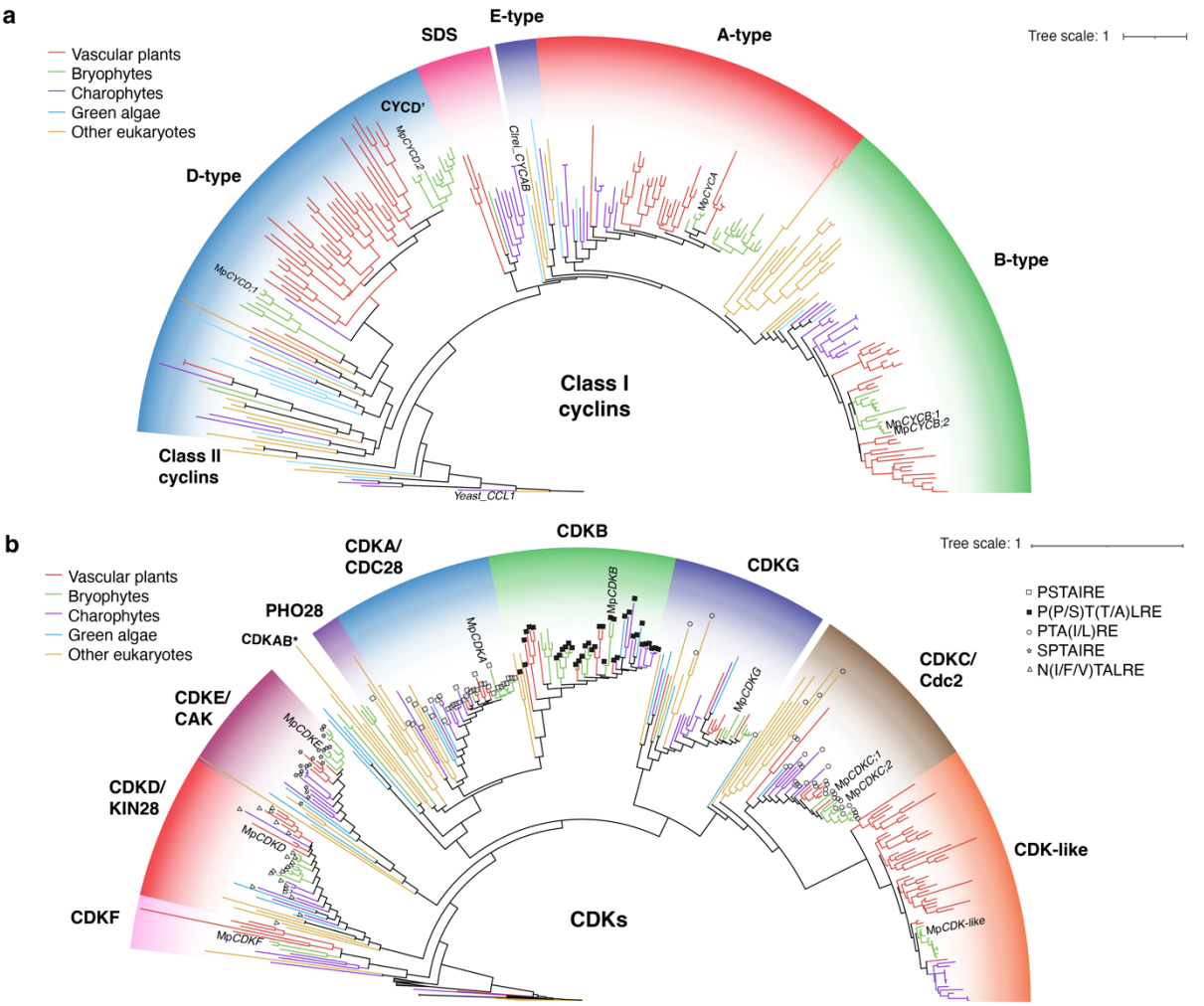

c

	Vascular plants												Bryophytes							Charophytes							Green algae			Other eukaryotes		
	A. thaliana	Sp. polyrhiza	Am. trichopoda	Ce. richardii	S. kraussiana	M. polymorpha	M. paleacea	L. cruciata	P. patens	Ce. purpureus	Takakia sp.	A. agresti	Z. circumcarinatum	P. margaritaceum	Me. endlicherianum	Cha. braunii	K. nitens	Chl. melkonianii	Me. viridae	O. lucimarinus	Chl. reinhardtii	Pra. coloniale	Cy. merolae	Ec. siliculosus	D. melanogaster	C. elegans	S. cerevisiae
CYCA	10	3	2	4	6	1	1	1	9	2	2	1	1	5	2	1	1	1	1	1	1*	1	0	1	3	1	0
CYCB	11	4	2	6	3	2	1	1	2	2	2	2	2	4	2	3	1	1	1	1	1*	1	1	2	2	4	6
CYCD	10	9	6	13	4	2	2	2	3	4	3	2	1	1	0	0	2	2	4	2	5	0	1	1	1	1	3
SDS	1	1	1	1	0	0	0	0	0	0	0	1	1	2	1	3	1	-	-	1	-	-	-	-	-	-	-
CYCE	-	-	-	-	-	-	-	-	-	-	-	-	-	-	-	-	-	-	-	-	-	1	1	0	1	2	-
CDKA/	1	2	2	6	1	1	1	1	2	3	1	2	1	3	1	1	1	1	2	1	1	1	1	0	2	1	1
CDKB	4	2	1	10	0	1	1	1	7	5	2	1	2	1	1	1	1	1	1	1	1	0	1	1	-	-	-
CDKAB*	-	-	-	-	-	3	2	-	-	-	-	-	-	-	-	-	-	-	-	-	4	-	-	-	1	2	-
PHO85	-	-	-	-	-	-	-	-	-	-	-	-	-	-	-	-	-	-	-	-	-	-	-	-	2	3	1
CDKC	2	1	1	2	3	2	2	1	3	1	1	2	1	0	1	2	1	1	1	1	1	0	1	3	2	2	1
CDK-like	16	6	7	9	2	1	1	1	4	2	1	1	1	3	1	1	1	-	-	-	-	-	-	-	-	-	-
CDKD	3	1	1	1	2	1	1	1	3	3	0	1	0	1	1	2	1	1	1	1	1	1	1	1	1	1	1
CDKE	1	1	1	1	1	1	1	1	2	1	1	1	0	1	0	1	1	1	1	1	1	1	0	0	1	1	2
CDKF	1	1	1	1	1	1	1	0	0	0	1	0	0	0	0	1	1	0	1	-	-	-	-	-	-	-	-
CDKG	2	2	1	1	2	1	0	1	2	2	2	2	1	1	1	0	1	1	2	2	2	0	0	1	3	2	0
CKS	2	1	2	5	2	1	1	1	6	1	2	2	1	6	2	1	2	1		1	1	1	1	3	2	2	1
RBR	1	1	1	1	1	1	1	1	4	2	1	1	1	3	1	1	1	1	1	1	1	1	1	1	2	1	0
E2F	3	2	2	3	2	1	1	2	4	2	1	1	0	1	1	0	1	1	1	1	1	1	1	1	2	3	0
DP	2	1	2	2	1	3	3	2	4	2	0	1	1	3	1	2	1	1	1	1	2	1	2	1	1	1	0
DEL	3	2	1	2	1	2	1	2	4	4	1	1	0	0	1	2	2	0	1	1	0	2	1	1	0	0	0
3R-MYB	5	5	4	2	2	8	3	2	2	2	1	1	2	0	1	1	1	2	1	1	0	1	1	6	1	0	0

Figure 1. Phylogenetic analysis of core cell cycle genes across eukaryotes. *a-b) Maximum likelihood Phylogenetic analysis of cyclins across representative plant and*

186 *eukaryotic species. (a) and CDKs (b). In each diagram, subfamilies are indicated with*
187 *different shaded background colours. Branches are coloured according to species in*
188 *each clade as shown in the figure legends. Conserved signature motifs across CDKs*
189 *are indicated in each node as shown in the figure key on the right. Full phylogenies*
190 *and details are available at Suppl. File 1. c) Summary of the number of cell cycle genes*
191 *across eukaryotic species. Background colour indicates the total number of genes in*
192 *darker red. Hyphens indicate absence, while red zeros indicate potential losses. **
193 *Chlamydomonas reinhardtii has an extra divergent CYCAB1 (Cre08.g370401).*

194

195 **Expression profile of cell-cycle genes in Marchantia**

196 To investigate the dynamic expression of key cell-cycle regulators in Marchantia, we
197 re-analysed RNA-seq time-series data from two natural biological processes that
198 feature a semi-synchronized re-entry to the cell cycle: meristem regeneration (Ishida
199 et al., 2022) and sporeling germination (Bowman et al., 2017). During regeneration,
200 cells begin proliferating approximately 16 hours after meristem excision (Nishihama et
201 al., 2015). Similarly, dormant spores start dividing between 29 and 48 hours after
202 exposure to light (Attrill et al., 2024).

203 During sporeling germination Mp*CYCD;1* transcripts accumulated after 24 hours of
204 light exposure, before the first cell division, followed by peaks in Mp*CYCB;1*, Mp*CYCA*,
205 Mp*CDKB*, Mp*CKS* at 48 hours (Figure 2a). We also employed *HISTONE H3.1*
206 (Mp*H3.1)* transcript accumulation as a reference marker for DNA replication, which
207 also peaked 48 hours after light exposure. A similar pattern was observed during
208 regeneration (Figure 2b), consistent with previous reports (Nishihama et al., 2015).
209 These findings are consistent with a role for Mp*CYCD;1* in G1, driving cell cycle re-
210 entry, and highlight other genes that are induced during cell cycle progression. On the
211 other hand, Mp*CDKA*, other CDKs, Mp*RBR,* and Mp*CYCD;2* remained constitutively
212 expressed (Figure 2, Suppl. Figure 1, Suppl. Figure 2). Mp*E2F* and Mp*DP1*
213 transcription factors showed moderate but detectable upregulation (Figure 1a-b).

214 Some predicted cell-cycle genes showed low or no detectable expression during both
215 regeneration and sporeling germination, including: Mp*CYCB;2, MpCDKAB;1-3,* and
216 Mp*DP2 MpDP3* (Figure 1, Suppl. Figure 1). Mp*3R-MYB1* remained the most

217 abundantly expressed *3R-MYB* ortholog in the vegetative gametophyte. By contrast,
218 Mp*3R-MYB3* to Mp*3R-MYB9* were specifically expressed during early sporophyte
219 development, and Mp*3R-MYB7* and Mp*3R-MYB8* were detected at the spore stage
220 too (Suppl. Figure 1). These 3R-MYB homologues belong to a different clade
221 compared to 3R-MYB1 expressed in the gametophyte (Suppl. Figure 1). Something
222 analogous was observed with Mp*DEL2*, which is expressed in the antheridium (Suppl.
223 Figure 1). These data suggest that in the vegetative gametophyte, a simplified cell
224 cycle regulation network is active, with only one copy of each TF. While in the
225 sporophyte and during gametogenesis, some specialization could be expected.

226 To further investigate the spatial distribution of cell divisions and growth, we focused
227 on the early stages of Marchantia gemma development. The meristem undergoes a
228 transition from an immature state to the fully mature state around 5-days post-
229 germination (Romani et al., 2024). We performed 5-ethynyl-2'-deoxyuridine (EdU)
230 staining to label actively dividing cells. As expected, EdU-positive cells were
231 concentrated around the division and differentiation zones (DDCZ) and the stem-cell
232 zone (SCZ), including the apical cell (Figure 2a-b). This is the main focal point for
233 growth in Marchantia, with a very simple architecture. Cells near the apical notch
234 proliferate and differentiate, forming specialized cells and air pore structures.
235 Epidermal cells exit the cell cycle and elongate as they become distal to the apical
236 notch (Figure 2a-b).

237 To elucidate the expression of cell cycle regulators during gemmaling development,
238 we generated transcriptional reporters using Golden-Gate compatible constructs
239 (Sauret-Gueto et al., 2020; Romani et al., 2024). Transcriptional reporters showed that
240 most key components were actively expressed in the EdU-positive zone (Suppl. Figure
241 3), corresponding to the DDCZ of the vegetative meristem. Consistent with the
242 transcriptomic analysis, the promoter of Mp*CYCB;2* showed no detectable expression,
243 suggesting it could be a pseudogene. *pro*Mp*CYCD;2* exhibited a more irregular pattern
244 compared to *pro*Mp*CYCD;1*, which was consistently expressed in dividing cells. TFs
245 linked to cell cycle regulation, including Mp*3R-MYB1*, and Mp*E2F,* followed expected
246 expression patterns based on prior transcriptomic analyses in the gametophyte
247 (Suppl. Figure 3). Expression of DP TFs reporters was not detectable at this stage
248 (Romani et al., 2024). This is inconsistent with Mp*DP1* transcriptomics, likely due to

249 the promoter being insufficient to capture all regulatory elements important for this
250 gene.

251

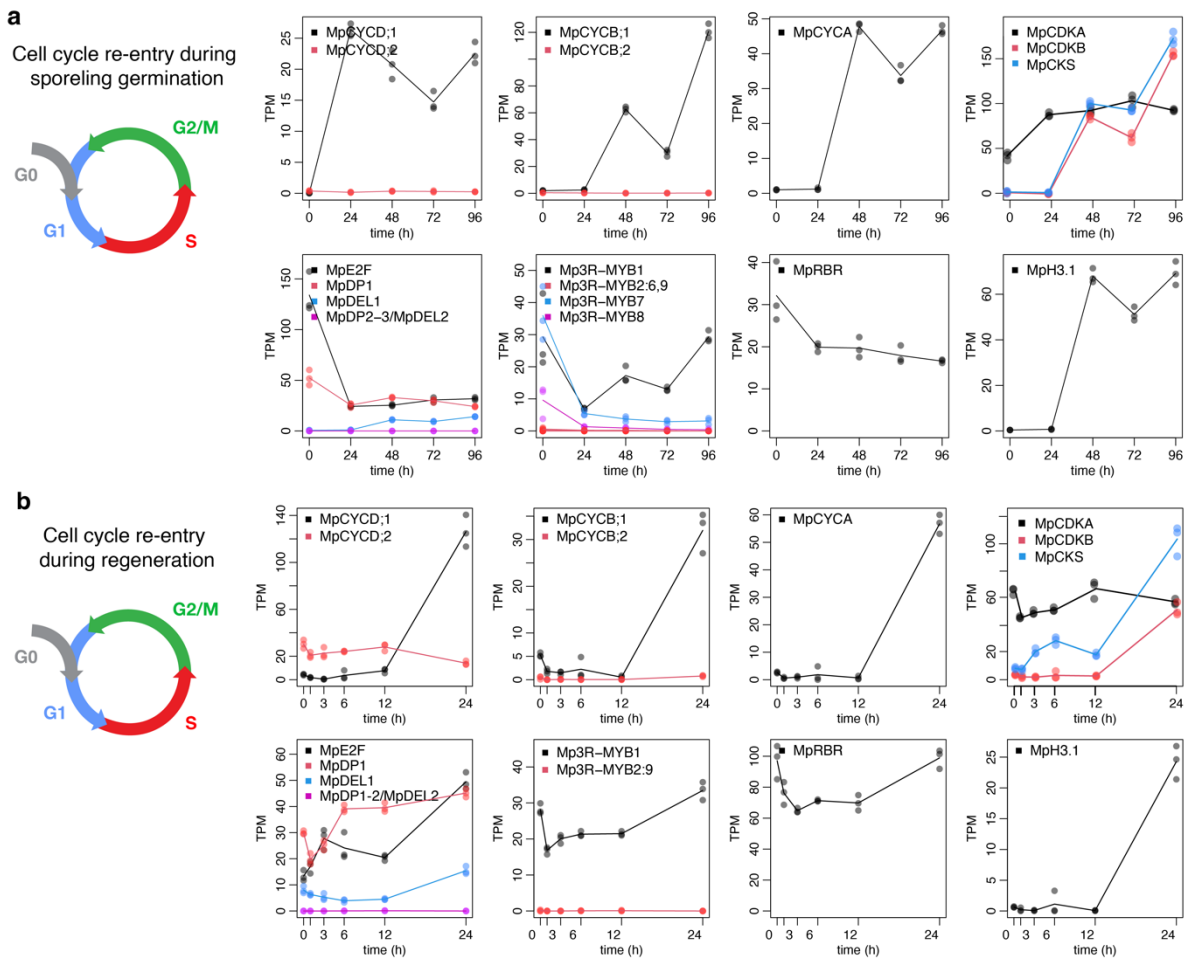

252

253 ***Figure 2. Expression of core cell cycle genes in Marchantia during re-entry.*** a-b)
254 *RNA-seq analysis of representative cell cycle genes during the time course of*
255 *sporeling germination (a) and regeneration (b). Genes are grouped per families and*
256 *distinguished by colour (see legend). Individual points represent biological replicates*
257 *and lines averages.*

258

259 **Phase specificity of cell-cycle genes**

260 To gain a more refined understanding of the dynamic expression of cyclins during all
261 phases of the cell-cycle, we leveraged single-cell RNA-seq data obtained from growing
262 gemmalings. Previous work identified clusters of cells proliferating around the apical

263 notch, including cell cycle related genes (Wang et al., 2023). Sub-clustering of this
264 group revealed three clearly distinct expression profiles (Figure 3c). Using well-known
265 markers, we labelled sub-clusters corresponding to G0/G1, S, and G2/M phases and
266 identified a comprehensive set of additional phase specific markers (Suppl. Table 1).
267 The G0/G1 sub-cluster was characterized by the expression of Mp*CYCD;1*, Mp*CDKA*,
268 and Mp*MCM3*, homologues of *Arabidopsis* G1-phase markers (Zhang et al., 2021)
269 and other genes associated G1 and initiation of replication (Figure 3c). The S-phase
270 cluster was defined by replication-related genes, including Mp*CYCA*, several histones,
271 and DNA damage repair genes such as Mp*RAD51*. The G2/M sub-cluster showed
272 elevated expression of mitotic markers, including the single CDH1 unit of the
273 Anaphase Promoting Complex/Cyclosome (APC/C) present in Marchantia
274 (Mp*CCS52A1),* both *CDC;20* cofactors (Mp*CDC20;1* and Mp*CDC20;2*) (Figure 2e-f),
275 and key core cell-cycle genes: Mp*CDKB,* Mp*CKS,* and Mp*3R-MYB1*. Among the other
276 CDKs, Mp*CDKD* showed differential expression in the G2/M cluster and Mp*CDKG* and
277 Mp*CDK-like* in G0/G1, similar to their homologues in *Arabidopsis* (Menges et al.,
278 2005). Transcript levels of other key components of the cell cycle such as RBR and
279 CKIs did not show preferred accumulation in specific phases of the cell-cycle.

280

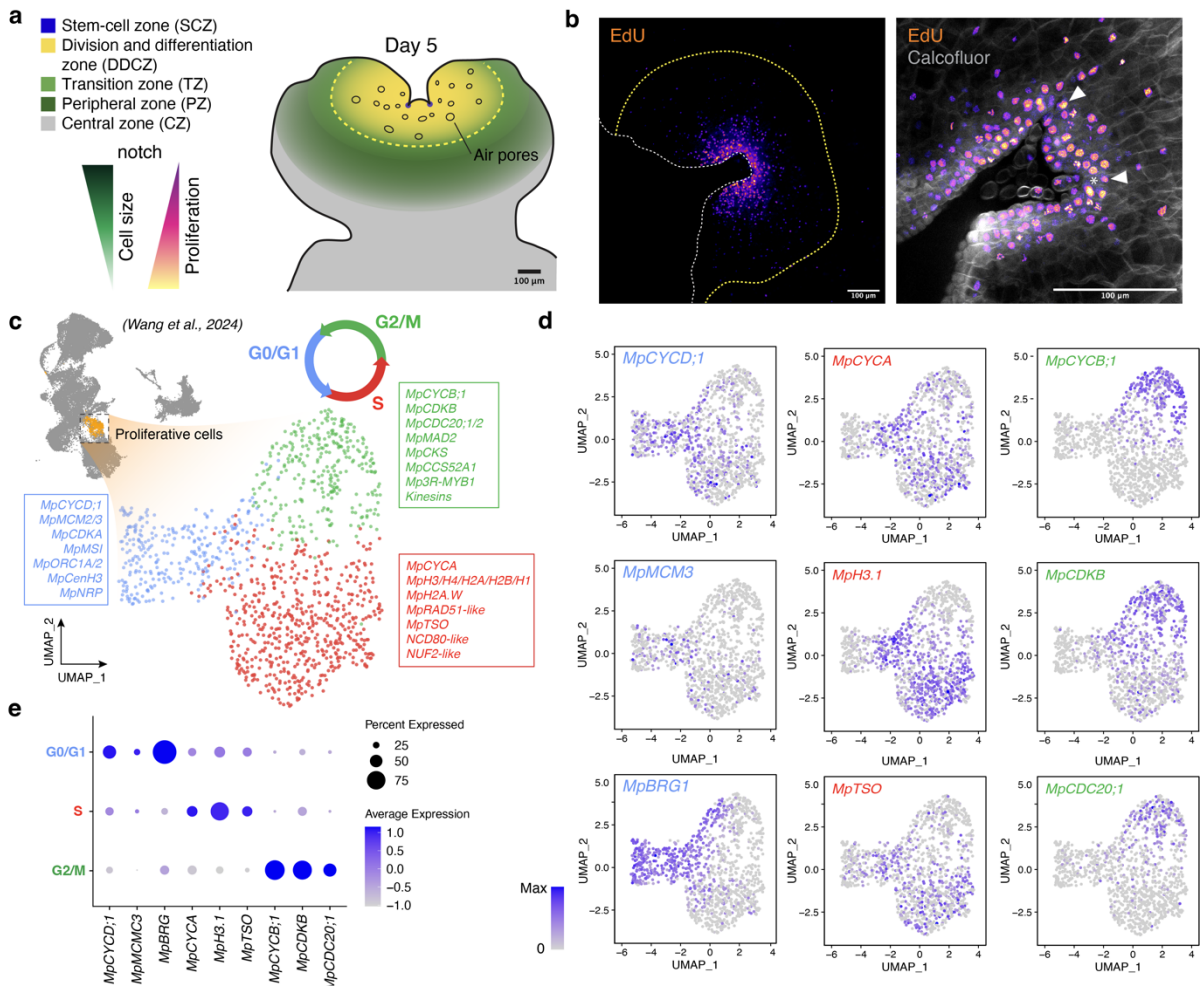

Figure 3. **Gene expression fluctuations during cell proliferation *in Marchantia.*** *a) Diagram of cellular domains associated with cell proliferation in the Marchantia gemmaling b)* 5-ethynyl- 2'-deoxyuridine (*EdU) staining of the Marchantia meristem in 5-days old gemmalings. The white dashed line delimitates the outline of the plant. The yellow dashed line represents the boundary of the mature epidermis.* Scale bar is shown in each image. *c-e)* UMAP of scRNA-seq of Marchantia proliferative cells subcluster. The UMAP including all cells is shown in the top left corner for reference. Proliferative cells are highlighted in orange. e) UMAP of the proliferative cells and classification into 3 sub-clustering (G0/G1, light blue; S, red; and G2/M, green). Feature plots (d) and dot plot (e) of representative genes are shown in coloured square legends. Abbreviations: *MCM (MINICHROMOSOME MAINTENANCE), CDC (CELL DIVISION CYCLE PROTEIN HOMOLOGUE), MSI (MUSASHI), ORC (ORIGIN RECONGNITION PROTEIN), CCS52A (CELL CYCLE SWITCH PROTEIN 52 A), NDC (NUCLEAR DIVISION CYCLE), NUF (KINETOCHORE PROTEIN NUF),*

296 *BRG (BLEOMYCIN RESISTANT GENE), NRP (NAP-RELATED PROTEIN). TPM,*
297 *transcripts per million; asinh, inverse hyperbolic sine.*

298

299 Cyclins are not only subjected to tight transcriptional control during cell division, but
300 also protein degradation. We made translational reporters for MpCYCD;1/2,
301 MpCYCB;1, MpCYCA and MpCDKA to better capture the protein expression dynamics
302 during cell division. These protein fusions correspond to the CDS and a C-terminal
303 mVenus fluorescent protein. Compared to promoter fusions for the corresponding
304 genes, the signals are more restricted to dividing cells. MpCYCD;1 is highly expressed
305 in dividing cells as expected, and rhizoid precursors and air pores (Figure 4a, Suppl.
306 Figure 4a). On the other hand, MpCYCD;2 translational reporter was undetectable in
307 vegetative tissues. MpCYCB;1 has the typical “salt and pepper” (Figure 4a) as
308 described in its homologues in flowering plants (Schnittger et al., 2002a). A similar
309 pattern was observed for MpCYCA (Figure 4a). MpCDKA translational reporter is
310 broadly expressed across the mature thallus and not restricted to dividing cells (Suppl.
311 Figure 5a). Finally, MpCDKB is more restricted to dividing cells (Suppl. Figure 5b).

312 For time-lapse imaging, we took advantage of cell cycle re-entry occurring during
313 regeneration, which allows a clear visualization of the cellular features associated with
314 its expression dynamics during cell division using the translational reporters. Live
315 imaging showed that MpCYCD;1 protein accumulated in the nuclei of cells before cell
316 division and was rapidly degraded before the start of the prophase (Figure 4a, Suppl.
317 Video 1). Similarly, MpCYCA also accumulated in the nuclei until the prophase and
318 was rapidly released to the cytosol and degraded (Figure 4b, Suppl. Video 2). Finally,
319 MpCYCB;1 was transiently expressed in the cytosol and accumulated during
320 metaphase/anaphase, and signal was rapidly lost before cell plate formation (Figure
321 4c, Suppl. Video 3). Intriguingly, MpCYCB;1 was re-localized to the nuclei before loss
322 of signal, likely due to degradation. The translocation of B-type cyclins during the
323 metaphase-anaphase has been well described in animal cells (Clute and Pines, 1999)
324 with the export of CYCB from the nucleus to the cytosol (Toyoshima et al., 1998). To
325 our knowledge, this is the first report of this type of translocation in plant cells.

326 We also looked at translational reporters for MpCDKA and MpCDKB. Both were
327 localized in the cytosol and nucleus and fluorescence was visible throughout the cell
328 cycle. While MpCDKA strongly accumulated in the interphase (Suppl. Figure 6a,
329 Suppl. Video 4), MpCDKB was found more prominent later in the prophase and during
330 mitosis (Suppl. Figure 6b, Suppl. Video 5). Overall, these results align with the
331 respective roles of the main cyclins and CDKS in Marchantia in the progression of the
332 cell cycle. This also highlights the importance of protein degradation and nuclear
333 export/import in controlling cyclin-dependent activity.

334

335

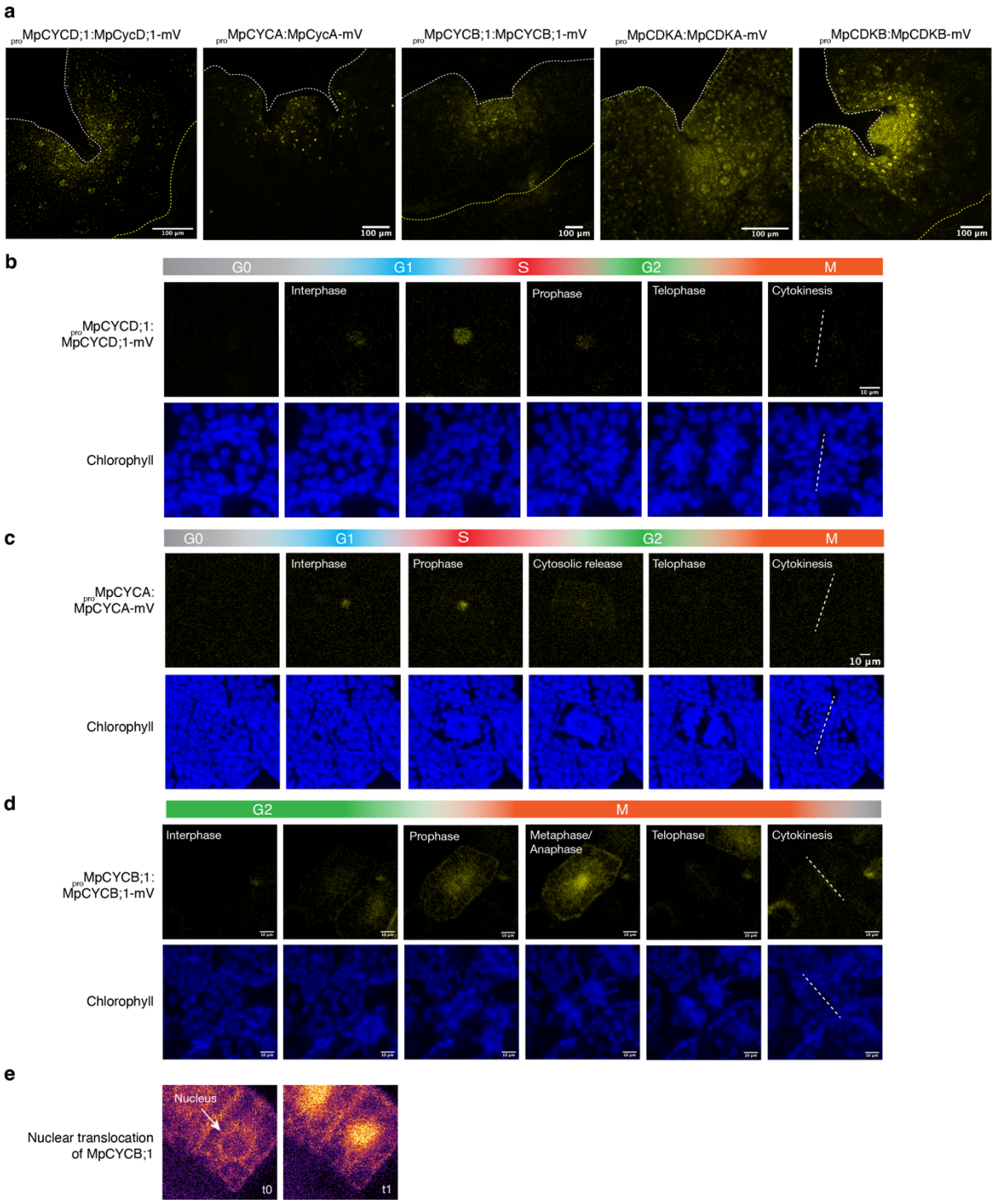

336

337 ***Figure 4. In vivo expression of cyclins and CDKs in Marchantia.*** Expression of
338 cyclin and CDKs translational reporters (yellow) in 5-days old gemmalings. b-d) Time-
339 lapse of MpCYCD;1 (b) MpCYCA (c), and MpCYCB;1 (d) translational reporters of an
340 individual cell dividing during regeneration (yellow). Chlorophyll (blue) is shown to
341 visualize the cell division phases using chloroplast movement. d) The translocation of

342 MpCYCB;1 (inferno LUT) from the cytosol to the nuclei at two different frames. The
343 full videos of the time-lapses are available at Suppl. Video 1-3. *The white dashed lines*
344 *delimit the outlines of the plants. The yellow dashed lines mark the boundary of the*
345 *mature.* Scale bars of the indicated sizes are shown in each image.

346

347 **Functional analysis of cyclins in Marchantia**

348 We generated fluorescent protein fusions (CDS-mVenus) for overexpression of cyclins
349 and CDKA. MpCYCD;1 is localized in the nucleus as most D-type cyclins in
350 *Arabidopsis,* while MpCYCD;2 showed a broader distribution in the cytosol (Figure
351 5a). As shown before, CDKA is cytosolic (Figure 5a) as its orthologue in *Arabidopsis*
352 (Boruc et al., 2010). Constitutive overexpression of Mp*CYCD;1* resulted in smaller
353 plants with reduced cell size and severe developmental defects (Figure 5b). In
354 contrast, overexpression of Mp*CYCD;2* or Mp*CDKA* had no noticeable effect on plant
355 growth (Figure 5c).

356 Mp*CYCB;1* and Mp*CYCB;2* share high sequence similarity (90.1 %), but Mp*CYCB;2*
357 lacks the conserved intron structure, and its endogenous expression is undetectable
358 (Figure 2, Suppl. Figure 1, Figure 5b). Both B-type cyclins localize in the cytosol and
359 nucleus (Figure 5a), consistent with its homologues in *Arabidopsis* (Boruc et al., 2010).
360 Overexpression of either Mp*CYCB;1* or Mp*CYCB;2* impaired growth, resulting in
361 smaller plants (Figure 5d). This indicates that despite signs of pseudogenization,
362 Mp*CYCB;2* encodes for a functional protein. Imaging of plants overexpressing
363 MpCYCB;1 revealed that cells with higher mVenus signal were arrested in mitosis at
364 a metaphase-like stage (Figure 5h, Suppl. Video 6), unlike the transient expression
365 observed native promoter control (Suppl. Video 7).

366 We also generated lines with inducible expression of Mp*CYCD;1*, Mp*CYCD;2*,
367 Mp*CYCB;1* Mp*CYCA* using an β-estradiol XVE system under the control of $_{pro}$MpE2F
368 (Siligato et al., 2016; Ishida et al., 2022). Inducible overexpression of MpCYCD;1
369 further confirmed its role in controlling cell division, producing ectopic cell division and
370 hyperplasia (Figure 5e,f), evidenced by significantly smaller cells under induction
371 (Figure 5g) lacking proper differentiation. Under this setting, inducible overexpression
372 of Mp*CYCD;2* did not cause any conspicuous developmental defect. On the other

373 hand, inducible overexpression of Mp*CYCB;1* caused cell death. Inducible expression
374 of Mp*CYCA* also caused a similar phenotype, suggesting that its accumulation is also
375 arresting cells at mitosis (Figure 5g). This supports the key role of Mp*CYCB;1* and
376 Mp*CYCA* in cell cycle control, while their degradation is required for the proper
377 progression of cytokinesis.

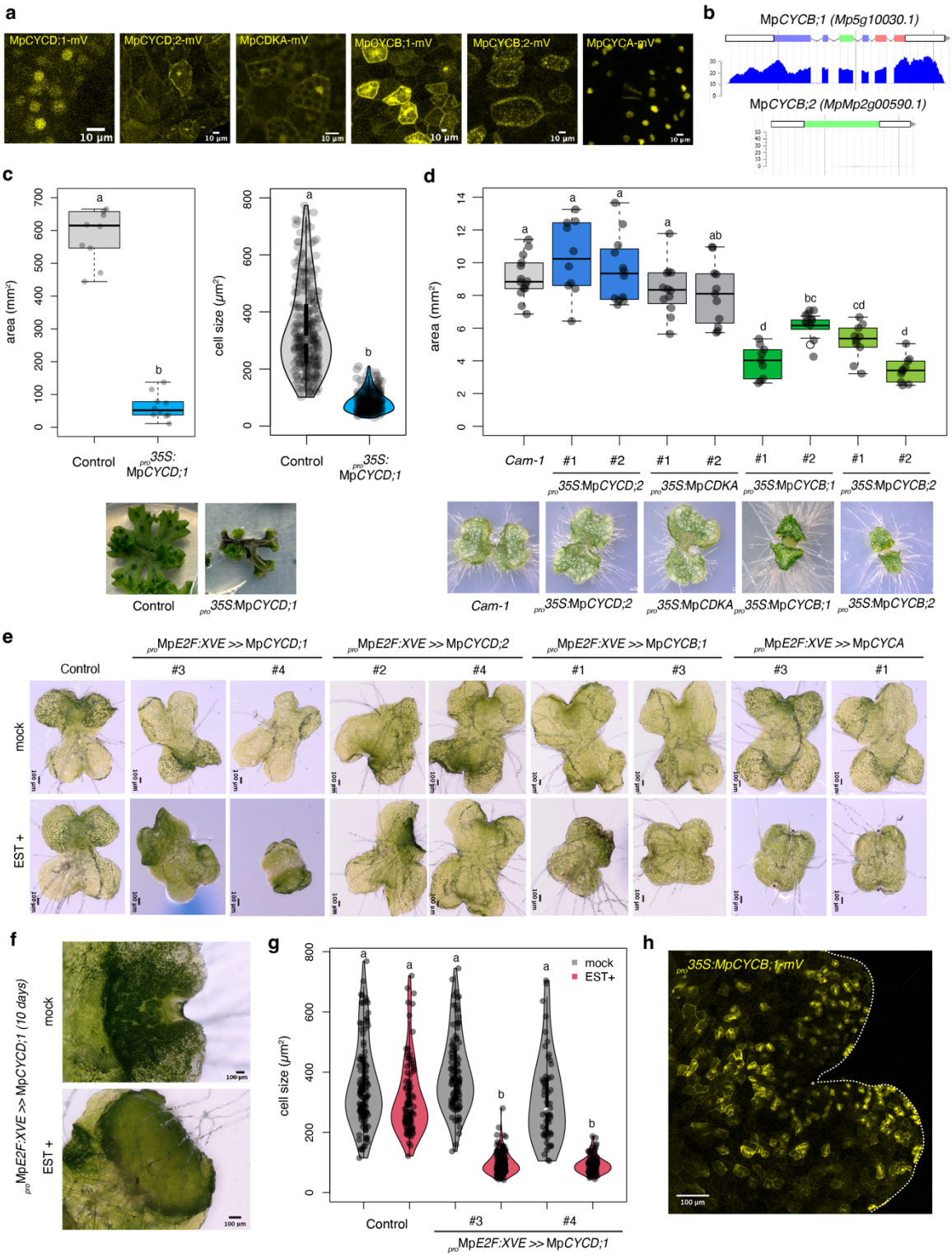

378

379 ***Figure 5. Functional characterization of cyclins and CDKA.*** *a) Subcellular*
380 *localization of selected cyclins and CDKA protein fusions with mVenus. b) Overview*
381 *of the genomic locus of* Mp*CYCB;1 and* Mp*CYCB;2, including a diagram of intron*
382 *structure and average RNA-seq coverage in mixed tissues. c) Boxplot of plant area*
383 *(left) and cell size (right) of* $_{pro}$*35S:*Mp*CYCD;1-mVenus primary transformant plants.*
384 *Representative pictures of the plants are shown. d) Boxplot of plant area of*
385 $_{pro}$*35S:*Mp*CYCD;2-mVenus,* $_{pro}$*35S:*Mp*CDKA-mVenus,* $_{pro}$*35S:*Mp*CYCB;1-mVenus,*
386 *and* $_{pro}$*35S:*Mp*CYCB;2-mVenus constitutive overexpression at 7 days. Representative*
387 *pictures of the plants are shown. e) Representative pictures of gemmalings of*
388 *transgenic plants with inducible overexpression of cylins grown for 3 days or 10 days*
389 *(f) in 0.5x Gamborg B5 supplemented with 5 µM β-estradiol (EST+) or DMSO (mock).*
390 *Transgenic constructs are indicated in the images. g) Violin plots of cell size of*
391 *inducible* Mp*CYCD;1 (*$_{pro}$*MpE2F:XVE>>MpCYCD;1). in 3-days old plants. f) Confocal*
392 *microscopy of* $_{pro}$*35S:*Mp*CYCB;1-mVenus (yellow) overexpression. The white dashed*
393 *line delimitate the outline of the plant. The yellow dashed line represents the boundary*
394 *of the mature epidermis. Control indicates a transgenic line transformed with an empty*
395 *vector.* Scale bar lengths are indicated in the pictures. Symbols above the bars
396 indicate grouping by P-value<0.001 in a Tukey's Honest Significant Difference
397 method.

398

399 **Cell Proliferation Interferes with Differentiation**

400 Morphological defects observed after Mp*CYCD;1* overexpression showed that cell
401 differentiation was disrupted when cell division was ectopically induced (Figure 5c,f).
402 To explore this interaction, we employed cell-type-specific promoters to target
403 differentiating cells, specifically rhizoid precursors and oil body cells (Sauret-Gueto et
404 al., 2020; Romani et al., 2024). Both cell types, identifiable by their reduced chlorophyll
405 content and distinct morphology, showed specific expression of Mp*CYCD;1* at the
406 gemma stage. Misexpression of Mp*CYCD;1* under a rhizoid specific promoter
407 ($_{pro}$*MpRSL3*) caused ectopic cell divisions, resulting in the eventual loss of rhizoids
408 (Figure 6). Similarly, misexpression in oil body cells ($_{pro}$*MpERF13*) triggered ectopic

409 divisions, leaving smaller, scattered oil body cells in the gemma (Figure 6). Notably,
410 these effects were not observed in Mp*CYCB;1* misexpression lines (Suppl. Figure 7).

411 During regeneration, both rhizoid precursors and oil body cells can undergo division
412 and regenerate an entire plant after cell reprogramming (Nagai, 1919; Romani et al.,
413 2024). De-differentiation of rhizoid precursors into epidermal cells is a normal
414 phenomenon in some dorsal but not in ventral rhizoid precursors (Romani et al., 2024).
415 The misexpression of Mp*CYCD;1* appears to extend this phenomenon, promoting
416 widespread de-differentiation across ventral and dorsal precursors, impacting the
417 emergence of rhizoids.

418

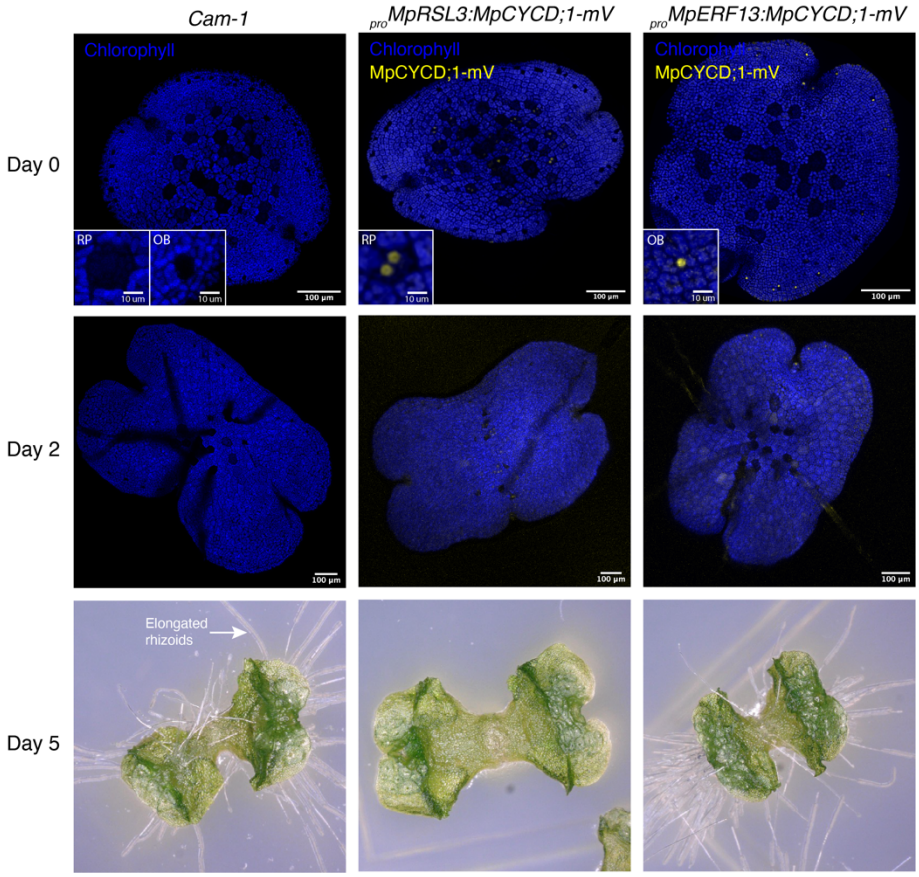

419

420 ***Figure 6. Cell-type specific overexpression of* Mp*CYCD;1 using cell-types***
421 ***specific promoters.*** Plants expressing *pro*Mp*RSL3*:Mp*CYCD;1-mVenus (rhizoid*
422 *precursor specific) and pro*Mp*ERF13*:Mp*CYCD;1-mVenus (oil body specific). Wild-type*
423 *Cam-1 was used as a control. Confocal full-stack images of representative individual*
424 *gemmalings (0, and 3) are shown with mVenus (yellow) and chlorophyll (blue)*

425 *channels merged. Representative picture of 5-days old gemmalings.* Scale bar lengths
426 are indicated in the pictures. *RP: rhizoid precursors. OB: oil bodies.*

427

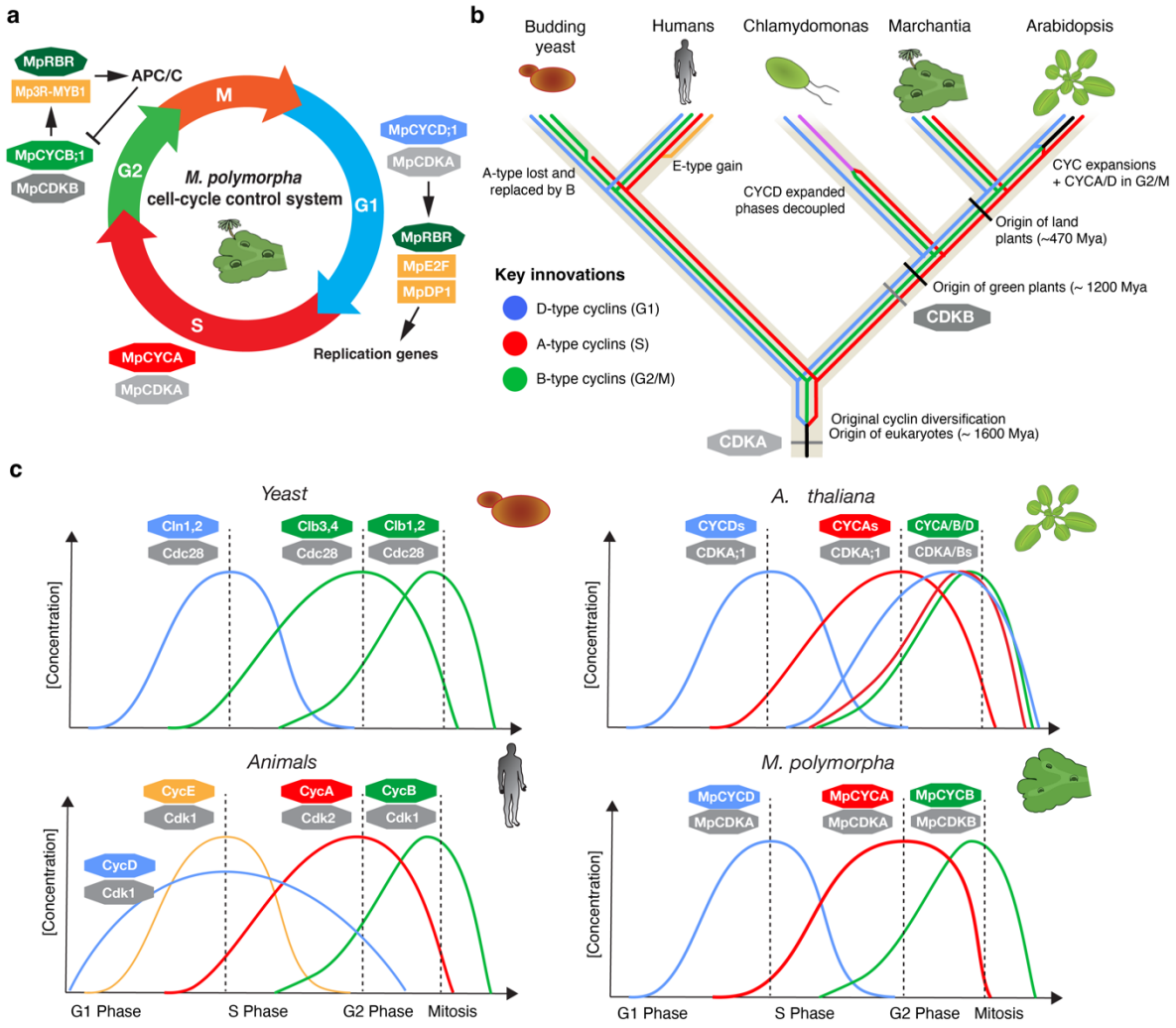

428

429 ***Figure 7. Core regulatory network of the cell cycle and phase specificity in***
430 ***Marchantia and other species***. *a) Diagram of cell cycle control system in Marchantia.*
431 *b) Phylogram of the evolutionary trajectory of cell cycle genes in model eukaryotes*
432 *(Saccharomyces cerevisiae, Homo sapiens, C. reinhartii, A. thaliana, and M.*
433 *polymorpha) and its possible ancestral state. c) Comparison of expression patterns of*
434 *cyclins and CDKs.*

435

436 **DISCUSSION**

437 We systematically characterised for the first time the functional integration of core cell-
438 cycle genes in Marchantia. The genetic simplicity of Marchantia is second to none
439 among plant model organisms, as its cell-cycle control system is neither expanded (as
440 in most eukaryotes) nor reduced (as in yeast). On the other hand, displays the main
441 features conserved among plants and has the potential to bridge the gap between
442 unicellular algae and flowering plants at the systems level.

443 We showed that Marchantia displays simple set of cell-cycle genes (Figure 1).
444 Particularly, the expression of cyclins follows an archetypal pattern with each gene
445 peaking at the corresponding phase of its putative function, resembling the cell cycle
446 regulation observed in animals and yeast. To achieve this, cyclin expression is tightly
447 controlled at the transcriptional (Figure 2) and posttranscriptional (Figure 3) levels. In
448 Marchantia this pattern is characterized by CYCD and CDKA during G1-phase, CYCA
449 during S-phase, and CYCB and CDKB in G2/M (Figure 7a). Based on phylogenetic
450 analysis and functional studies in Marchantia and other species, it can be inferred that
451 this simple configuration represents the ancestral state of cell cycle regulation in
452 eukaryotes, except for CDKB being specific to plants (Figure 7b).

453 The streamlined system of cyclin-CDK components in Marchantia indicates that a
454 complex regulatory network is not a prerequisite for multicellularity in plants but rather
455 a derived feature in flowering plants. Thus, the extensive cyclin diversity observed in
456 vascular plants likely arose through lineage-specific gene duplications, leading to
457 redundancy and diversification. Subsequent neofunctionalization and
458 subfunctionalization, may have facilitated cellular innovations and tissue specificity. In
459 contrast, the set of key regulators that we described here for Marchantia are expressed
460 in both the haploid and diploid generation (Suppl. Figure 1). This might imply that a
461 very similar machinery controls cell division across both generations and meiosis, with
462 few specific features.

463 The only two gene duplications among Class I cyclins in Marchantia, Mp*CYCB;2* and
464 Mp*CYCD;2,* do not appear to play significant roles in cell cycle regulation. Mp*CYCB;2*
465 is likely a pseudogene with negligible expression, while Mp*CYCD;2* is not a canonical
466 D-type cyclin (due to its subcellular localisation and overexpression phenotype).

467 Instead, it belongs to a novel clade of bryophyte specific D-type cyclins (CycD'), which
468 function remains to be elucidated.

469 Determining the truly essential components for the cell cycle progression remains a
470 challenge across eukaryotes. While CDKA plays a central role across eukaryotes, it is
471 not strictly essential in *Arabidopsis, Physcomitrium, and Chlamydomonas* (Nowack et
472 al., 2012; Tulin and Cross, 2015; Bao et al., 2022). In Marchantia, CDKA is steadily
473 expressed in dividing cells, with some preference for G1 (Figure 3), and does not
474 appear to be a rate-limiting factor (Figure 5). CDKB, a G2/M-specific innovation
475 conserved across green plants, is essential for spindle formation and nuclear division
476 in *Chlamydomonas* (Tulin and Cross, 2014; Pecani et al., 2022). Our results suggest
477 that MpCDKB is highly expressed at G2/M, likely interacting with MpCYCB;1.
478 However, CDK protein levels are detected throughout the cell cycle and do not exhibit
479 the strict phase-specific posttranscriptional regulation observed for cyclins.

480 D-type cyclins are conserved across eukaryotes and are undoubtedly important for
481 plant growth and development, though their essentiality in plants remains unclear
482 (Cross and Umen, 2015). Overexpression of Mp*CYCD;1* in Marchantia produces
483 phenotypes similar to those observed for *CYCD3* homologs in flowering plants
484 (Dewitte et al., 2003; Koroleva et al., 2004; Menges et al., 2006), reinforcing the idea
485 that regulating cell cycle re-entry is the ancestral role of D-type cyclins in plants. This
486 is important to understand the divergent roles of other D-type cyclins in flowering
487 plants, and contrast with the role of D-type cyclins in animals (Datar et al., 2000).

488 We also demonstrated a close relationship between cyclin-mediated cell cycle re-entry
489 and cellular differentiation in Marchantia (Figure 6). Our findings suggest that
490 maintaining proper coordination of cell division rates is essential for preserving cell
491 identity. This contrasts with Arabidopsis, where manipulating the cell cycle in
492 specialized cells, such as trichomes, alters cell size and induces multicellularity but
493 maintain cell identity (Schnittger et al., 2002b; Schnittger et al., 2002a). These
494 differences may help explain Marchantia's remarkable regenerative capacity and
495 developmental plasticity (Nishihama et al., 2015).

496 Interestingly, overexpression of Mp*CYCA* or Mp*CYCB* is deleterious in Marchantia,
497 leading to cell cycle arrest. In the case of A-type cyclins, they are usually associated

498 with ploidy level and control of S-phase duration in plants (Imai et al., 2006). However,
499 this might not be the case in Marchantia and other non-seed plants due to the absence
500 of endoreduplication (Bainard et al., 2013; Nishihama et al., 2015). In
501 *Chlamydomonas*, CYCA plays a critical role in cell division, but it is not essential
502 (Atkins and Cross, 2018). It was also shown that overexpression of *CYCA3* in
503 Arabidopsis cyclins affect meristem activity (Takahashi et al., 2010; Willems et al.,
504 2020). Given that Arabidopsis *CYCA3* cyclins are also expressed at the S phase as
505 MpCYCA in Marchantia. This suggest that controlling cell cycle progression during the
506 S phase could be the ancestral role for A-type cyclins across plants. Subsequently,
507 the role in ploidy could be restricted to the *CYCA2* clade and meiosis to *CYCA1* clade
508 (d'Erfurth et al., 2010).

509 In the case of B-type cyclins, both function and phase specificity are well conserved
510 across eukaryotes, playing a key role in regulating the G2/M transition, as we showed
511 in Marchantia. Their essentiality for cell division was demonstrated in *Chlamydomonas*
512 (Pecani et al., 2022). Historically, overexpression of *CYCB* is often associated with
513 higher division rates (Doerner et al., 1996). However, in Marchantia, overexpression
514 of Mp*CYCB;1* or Mp*CYCA* did not increase division rates but instead caused mitotic
515 arrest. This arrest may result from the inability of some cells to degrade excessive
516 cyclins, thereby preventing progression through mitosis (Figure 5h). The expression
517 of non-degradable CYCBs in plants and other eukaryotes has also been shown to
518 cause mitotic arrest, supporting that their degradation by the APC/C is critical (Figure
519 6). Similarly, A-type cyclins also need to be degraded by the APC/C but prior to the
520 spindle assembly checkpoint in other eukaryotes (Geley et al., 2001). Our results
521 suggest that *CYCA* degradation is also critical for cell-cycle progression in plants too
522 (Figure 5).

523 It remains an open question whether A- or B-type cyclins are limiting factors for growth
524 in Marchantia, as has been observed in other plants (Doerner et al., 1996). A possible
525 explanation is that the balance between cell division or arrest is highly dose
526 dependent. In addition to their role in mitotic control, CYCB1;1 induction in Arabidopsis
527 has also been shown to cause mitotic arrest under DNA damage conditions
528 (Schnittger and De Veylder, 2018). In animals, B-type cyclins are also not rate limiting
529 for cell proliferation (Doonan and Hunt, 1996), suggesting that this could represent the

530 ancestral state of CYCB protein function in eukaryotes. However, further studies are
531 required to generalize the precise functions of A- and B-type cyclins in plants.

532 On the other hand, we showed that MpCYCD;1 is the single rate-limiting cyclin/CDK
533 component for cell proliferation in Marchantia. Unlike MpCYCA and MpCYCB;1, its
534 degradation may not be required for mitotic progression. Rather, its accumulation
535 triggers re-entry into G1 and may be crucial for integrating developmental and
536 environmental signals to regulate plant growth rate.

537 The role of the DREAM complex TFs (E2F/DP and 3R-MYBs) is also important to
538 shape the downstream signalling networks of the cell cycle. The Marchantia genome
539 encodes homologs of these regulators, but only one copy of each component is
540 expressed in the gametophyte. The single-copy nature of E2F TFs in Marchantia and
541 other land plants suggests that the complexity observed in Arabidopsis and animals
542 arose independently (Sozzani et al., 2006; Rauber et al., 2016). The diversification of
543 3R-MYBs appears to be ancestral to land plants, and their expansion in Marchantia
544 may be linked to sporophyte-specific programs (Supplementary File 1).

545 In conclusion, Marchantia provides a valuable model for studying cell cycle to
546 demonstrate general principles of growth regulation that could be applied to complex
547 organisms. Further studies using conditional knockouts (Nishihama et al., 2016) could
548 clarify the roles of specific cell cycle genes in land plants. Additionally, targeted
549 investigations into how environmental stress, DNA damage, hormones, or mechanical
550 cues influence cell cycle progression will further enhance our understanding. The
551 foundational work presented here establishes a toolkit of genes and promoters that
552 can be leveraged for biotechnological applications. A deeper understanding of the cell
553 cycle will enable more precise approaches to reprogramming plant growth and
554 development.

555

556 **ACKNOWLEDGEMENTS**

557 This work was funded by BBSRC BB/T007117/1 to J.H, and BBSRC BB/F011458/1
558 for confocal microscopy. F.R. is a Leverhulme Early Career Fellow (ECF-2023-534)
559 funded by the Leverhulme Trust and the Isaac Newton Trust (23.08(f)), I.B. is funded

560 by the Herschel Smith Fund studentship. We thank Miguel A. Blazquez and Antonio
561 Serrano Mislata (IBMCP, Valencia, Spain) for useful discussion and feedback on the
562 manuscript. We thank Jia-Wei Wang and Long Wang (CAS, China) for advice and
563 help on scRNA-seq data analysis.

564

565 **MATERIAL AND METHODS**

566 **Phylogenetic analysis**

567 *Ceratopteris richardii* v2.1 (Marchant et al., 2022), *Amborella trichopoda* v1.0
568 (Amborella Genome, 2013), *Chlamydomonas reinhardtii* v5.5 (Merchant et al., 2007),
569 *Physcomitrium patens* v6.1 (Bi et al., 2024) and *Spirodela polyrhiza v2* (Wang et al.,
570 2014) proteomes were obtained from Phytozome. *Phaeodactylum tricornutum*
571 ASM15095 v2 (Bowler et al., 2008), *Prasinoderma coloniale* v1.1 (Li et al., 2020b),
572 *Ostreococcus lucimarinus* ASM9206 v1 (Palenik et al., 2007), *Mesotaenium*
573 *endlicherianum* v2 (Cheng et al., 2019), *Mesostigma viridea* (Liang et al., 2020)(ref),
574 *Ectocarpus siliculosus (Cock et al., 2010)*, and *Chara braunii* v1.0 (Nishiyama et al.,
575 2018) proteomes were obtained from Phycocosm. *Saccharomyces cerevisiae* R64.1.1
576 (Goffeau et al., 1996), *Caenorhabditis elegans (Consortium, 1998)*, and *Drosophila*
577 *melanogaster* BDGP6.46 (Adams et al., 2000) proteomes were obtained from
578 Ensembl, and *Cyanidioschyzon merolae* ASM9120 v1 (Matsuzaki et al., 2004) was
579 obtained from Ensembl Plants. The proteomes from *Marchantia polymorpha Tak* v6.1
580 (Montgomery et al., 2020), *Selaginella kraussiana* v2 (Liu et al., 2023), *Anthoceros*
581 *agresti* Oxford (Li et al., 2020a), *Klebsormidium nitens* NIES-2285 (Hori et al., 2014),
582 *Zygnema circumcarinatum* (Feng et al., 2024), *Penium margaritaceum* (Jiao et al.,
583 2020), *Marchantia paleacea* (Radhakrishnan et al., 2020), *Lunularia cruciata* v1 (Linde
584 et al., 2020) from their respective sources.

585 Hidden Markov Models matrix for PFAMs including cyclins (PF00134.28), CKS
586 (PF01111.24), E2F (PF02319.25), and RBR (PF01858.22) were used as query for
587 searching using hmmsearch function from HMMER v3.4 (Finn et al., 2011). The cut-
588 off E-value was then adjusted aiming to have 100% sensitivity for annotated genes
589 and exclude low confidence findings: Cyclins < 1E-10, CKS < 1E-10, E2F < 1E-5, RBR
590 < 1E-50. Using the hmmsearch output, Seqinr in R (Charif and Lobry, 2007) package
591 was to retrieve the sequences from the proteomes.

592 3R-MYBs proteins were BLASTed using the human MYBB sequence as a query
593 (threshold E-value < 2e-34) aiming to have 100% sensitivity for annotated 3R-MYB
594 and include some R2R3-MYBs. Similarly, for CDK proteins, using yeast CDC28 and
595 Arabidopsis CDKF as query (threshold E-value < 1e-44) aiming to have 100%

596 sensitivity for annotated CDKs. Sequences were extracted from the proteomes using
597 Biostrings package in R (Lifschitz et al., 2022).

598 Finally, JalView (Procter et al., 2021) was used to align sequences with the MAFFT
599 software (Katoh et al., 2002) and trimming the alignment to include only columns with
600 50% coverage. Maximum-likelyhood phylogenetic analysis was performed using
601 IQtree 2 (Minh et al., 2020) with default parameters. Trees were rooted and visualised
602 using iTOL v6 (Letunic and Bork, 2024). Complete trees available at (Suppl. File 1).

603 To count the number of MYB repeats (SM00717) for 3R-MYB proteins, we used
604 InterProScan (Quevillon et al., 2005). To identify signature motifs on CDKs we used a
605 simple grepl search function. Marchantia genes names were annotated in
606 MarpolBase.

607

608 **Analysis of public RNA-sequencing data**

609 TPM values for sporeling germination and different developmental stages were
610 extracted from Marpolbase Expression database (Kawamura et al., 2022) or
611 downloaded from SRA for regeneration (DRR330148- DRR330173), mapped in *M.*
612 *polymorpha* Tak-1 genome v5.1 using HISAT2 (Kim et al. 2019), ht-seq and EdgeR.
613 Data was subsequently analysed with R to generate plots using customs scripts.
614 Heatmap was generated using Marpolbase Expression database (Kawamura et al.,
615 2022).

616 The scRNA-seq matrix for Marchantia gemmaling development (Wang et al., 2023)
617 was extracted from Beijing Institute of Genomics Data Center (OMIX004749) and re-
618 analysed using Seurat V5 package in R (Hao et al., 2024). Briefly, the dataset was
619 subseted to only cluster 10 and analysed with the following functions and parameters:
620 FindNeighbours (dims = 1:100, k.param = 200), FindClusters, RunUMAP (reduction =
621 'pca', metric = 'correlation', n.neighbours = 30L, dims = 1:100). Data was visualized
622 using DimPlot, FeaturePlot and DotPlot functions. Markers in Suppl. Table S1 was
623 obtained using FindAllMarkers function and genes annotated using MarpolBase.

624

625 **Plant material and growth conditions**

626 *Marchantia polymorpha* subs. *rudelaris* accessions *Cam-1* (male) and *Cam-*
627 *2* (female) were used in this study (Delmans et al. 2017). Under normal conditions,
628 plants were grown on solid 0.5× Gamborg B-5 basal medium (Phytotech #G398) at
629 pH 5.8 with 1.2% (w/v) agar micropropagation grade (Phytotech #A296), under
630 continuous LED light at 21 °C with light intensity of 150 μmol/m^2/s (Systion #SE-EGB).
631 For spore production, plants were grown in Microbox micropropagation containers
632 ($SacO_2$) in long-day conditions (16 h light/8 h dark) under light supplemented with far-
633 red light as described (Sauret-Güeto et al. 2020).

634

635 **Cloning and plant transformation**

636 To generate new L0 parts, CDS and promoter regions from genes were extracted from
637 *M. polymorpha* Tak-1 genome version 5.1 (Bowman et al. 2017) genome and manually
638 domesticated to remove internal BsaI and SapI sites using synonymous mutations for
639 the CDS. The sequences of synthetic L0 parts used in this work are available in Suppl.
640 Table S2. L0 parts were synthesized by GENEWIZ following the standard syntax for
641 plant synthetic biology with CDS and PROM5 or PROM and 5UTR overhangs and
642 cloned into the plasmid pUAP1 (Addgene #63674) (Patron et al. 2015) by homology
643 recombination. Other parts were derived from previous works (Sauret-Gueto et al.,
644 2020; Romani et al., 2024) as specified in Suppl. Table S2.

645 The acceptor pBy01 (Romani et al., 2024) was used to assemble using L0
646 corresponding to PROM5 or PROM and 5UTR parts and pBy10 (Tse et al., 2024) for
647 entire cassettes containing a hygromycin resistant cassette for plant selection. These
648 acceptors are binary vectors contain a LacZ selection cassette flanked by BsaI sites
649 to clone final vectors in one-step using L0 parts following the standard syntaxis (Patron
650 et al., 2015). Following the same logic, a new custom acceptor for chlorosulfuron
651 selection was generated based on pBy10 and OP-62 (Sauret-Gueto et al., 2020;
652 Romani et al., 2024). Another two custom acceptors were generated for cloning only
653 CDS with the $_{pro}$*35S* (pBy12) or estradiol inducible system using $_{pro}$*MpE2F:XVE* driving
654 the expression of $_{pro}$*LexA,* similar to previous published Gateway acceptor
655 pMpGWB168 *(Ishida et al., 2022)* and a $_{3utr}$*NOS* terminator, containing also an
656 hygromycin (pBy13) or chlorosulfuron (pBy23) resistant cassette for plant selection.

657 The full-length of the final constructs were verified by sequencing using the Oxford
658 Nanopore technology (Plasmidsaurus Inc.). The final plasmid map is provided in the
659 supplementary data (Supplemental File 2-3).

660 Plasmids were assembled as detailed in Suppl. Table S2 using Type-IIS cloning as
661 described previously for L3 plasmids (Romani et al., 2024). Briefly using a Master Mix
662 containing 10% (v/v) 10× T4 DNA ligase buffer (NEB #M0202), 5% (v/v) T4 DNA ligase
663 at 400 U/µL (NEB #M0202), 5% (v/v) BsaI at 20 U/µL (NEB #R3733), 10% (v/v)
664 acceptor at 40 ng/µL, 20% (v/v) pre-mixed L0 parts (~100 ng/µL) and water to a final
665 volume of 5 µL. Cycling conditions were 26 cycles of 37 °C for 3 min and 16 °C for 4
666 min. Termination and enzyme denaturation: 50 °C for 5 min, and 80 °C for 10 min.
667 Other L1 and L2 plasmids were cloned as described before (Sauret-Gueto et al.,
668 2020). TOP10 chemically competent *Escherichia coli* cells were transformed using the
669 assembly reaction and plated on LB-agar plates containing the corresponding
670 antibiotic and 40 µg/mL of 5-bromo-4-chloro-3-indolyl β-D-galactopyranoside (X-Gal).
671 The presence of the correct insert was confirmed by restriction XhoI digestion (Thermo
672 Scientific #FD0694) and Sanger sequencing using primers Fw5 (5′-
673 tactcgccgatagtggaaacc) and Rv5 (5′-aagcactgcaggccgtagcc-3′).

674 *Agrobacterium tumefaciens* (GV3101) cells were transformed using the freeze-thaw
675 method and used for plant transformation of Cam-1/2 spores as described in detail in
676 Annese et al., (2024). Plants were screened for positive fluorescence and at least two
677 independent lines were selected. For expression markers, only representative lines of
678 the 4-5 lines consensus expression pattern.

679

680 **Plant phenotyping**

681 Representative images of Marchantia plants were taken using a Keyence VHX-5000
682 digital microscope equipped with a 20x-200x Ultra-Small, High-Performance Zoom
683 Lens (VH-Z20R/Z20T). Thallus area was quantified from pictures (normally 7-days
684 old gemmalings) with ImageJ software with at least 10 biological replicates. Cell
685 sizes were quantified from manual segmentation of cells in 200x pictures using
686 ImageJ. Only cells surrounding the DDCZ but excluding smaller cells closer to the

687 apical meristem. At least 50 cells were measured for each biological replicate in at
688 least 3 biological replicates.

689 For β-estradiol (#E8875, Merck) treatments, a 50 mM stock was dissolved in DMSO
690 and added to melted agar-Gamborg B-5 media at a final concentration of 5 μM as
691 described in Ishida et al., (2021). Plants were grown in microscopy contact plates
692 and visualized after 3 or 10 days in normal growth conditions.

693

694 **Laser scanning confocal microscopy**

695 Confocal images of Marchantia were acquired on a Leica SP8X spectral confocal
696 microscope upright system equipped with a 460 to 670 nm super continuum white light
697 laser (80% laser power), two CW laser lines 405, and 442 nm, and 5 Channel Spectral
698 Scanhead (four hybrid detectors and one photomultiplier). For slides, imaging was
699 conducted using either a 10× air objective (HC PL APO 10×/0.40 CS2) or a 20× air
700 objective (HC PL APO 20×/0.75 CS2). When observing fluorescent protein with
701 overlapping emission spectra, sequential scanning mode was selected. Excitation
702 laser wavelength and captured emitted fluorescence wavelength window were: for for
703 mVenus (514 nm, 527 to 552 nm), and for chlorophyll autofluorescence (633, 687 to
704 739 nm).

705

706 **Time-course and time-lapses**

707 When imaging time-courses, plants grown under normal culture conditions in small
708 petri dishes, removed the lid for imaging, and returned the plants to the growth
709 chamber and imaged as described above. For live imaging, six stacked Gene Frames
710 (#AB0578, ThermoFisher) were placed on a glass slide and filled halfway with molten
711 Gamborg B-5 agar medium. Plants were then placed on the solidified agar surface
712 and meristems were removed using a Laser Microdissection Leica LMD7000.
713 Samples were mounted in perfluorodecalin (Littlejohn et al. 2010) with a glass
714 coverslip on top. The slides were then continuously imaged on the Leica SP8X
715 confocal microscope for 1 to 4 d.

716

717 **EdU staining**

718 5-days old gemmalings were incubated in liquid half-strength Gamborg's B-5 medium
719 under continuous light for 3 h with 20 µM 5-ethynyl- 2'-deoxyuridine (EdU) from the
720 Click-iT EdU Imaging Kit with Alexa Fluor 488 (#C10337, Invitrogen). Then they were
721 fixed with 4% formaldehyde for 1 h, washed twice with phosphate buffer saline (PBS)
722 and 0.5% Triton X-100 in PBS for 20 min. After washes, samples were incubated with
723 a freshly prepared reaction mixture following the manufacturer instructions but without
724 the Hoechst 33342 component. After staining, samples were protected from light,
725 washed twice with PBS and soaked in iTomei-D (#T3940, Tokyo Chemical Industry)
726 clearing solution as described before (Sakamoto et al., 2022). Samples were mounted
727 in perfluorodecalin (#130041000, ThermoScientific) (Littlejohn et al. 2010) with a glass
728 coverslip on top and imaged on the Leica SP8X confocal microscope as described
729 before.

730

731 **Statistics**

732 To obtain plots and statistical analysis, data was processed using R xv 4.4.1 software.
733 For average and boxplots, the stats package was used with default parameters. For
734 violinplots, the vioplot package was implemented also with default parameters.
735 Statistical significance was calculated using ANOVA using the stats package Tukey
736 'Honest Significant Difference' method (alpha = 0.05) for levels calculations.

737

738 **REFERENCES**

739 **Adams, M.D., Celniker, S.E., Holt, R.A., Evans, C.A., Gocayne, J.D., Amanatides,**
740 **P.G., Scherer, S.E., Li, P.W., Hoskins, R.A., Galle, R.F., George, R.A., Lewis,**
741 **S.E., Richards, S., Ashburner, M., Henderson, S.N., Sutton, G.G., Wortman,**
742 **J.R., Yandell, M.D., Zhang, Q., Chen, L.X., Brandon, R.C., Rogers, Y.H., Blazej,**
743 **R.G., Champe, M., Pfeiffer, B.D., Wan, K.H., Doyle, C., Baxter, E.G., Helt, G.,**
744 **Nelson, C.R., Gabor, G.L., Abril, J.F., Agbayani, A., An, H.J., Andrews-**
745 **Pfannkoch, C., Baldwin, D., Ballew, R.M., Basu, A., Baxendale, J.,**
746 **Bayraktaroglu, L., Beasley, E.M., Beeson, K.Y., Benos, P.V., Berman, B.P.,**
747 **Bhandari, D., Bolshakov, S., Borkova, D., Botchan, M.R., Bouck, J., Brokstein,**
748 **P., Brottier, P., Burtis, K.C., Busam, D.A., Butler, H., Cadieu, E., Center, A.,**
749 **Chandra, I., Cherry, J.M., Cawley, S., Dahlke, C., Davenport, L.B., Davies, P.,**
750 **de Pablos, B., Delcher, A., Deng, Z., Mays, A.D., Dew, I., Dietz, S.M., Dodson,**

K., Doup, L.E., Downes, M., Dugan-Rocha, S., Dunkov, B.C., Dunn, P., Durbin, K.J., Evangelista, C.C., Ferraz, C., Ferriera, S., Fleischmann, W., Fosler, C., Gabrielian, A.E., Garg, N.S., Gelbart, W.M., Glasser, K., Glodek, A., Gong, F., Gorrell, J.H., Gu, Z., Guan, P., Harris, M., Harris, N.L., Harvey, D., Heiman, T.J., Hernandez, J.R., Houck, J., Hostin, D., Houston, K.A., Howland, T.J., Wei, M.H., Ibegwam, C., Jalali, M., Kalush, F., Karpen, G.H., Ke, Z., Kennison, J.A., Ketchum, K.A., Kimmel, B.E., Kodira, C.D., Kraft, C., Kravitz, S., Kulp, D., Lai, Z., Lasko, P., Lei, Y., Levitsky, A.A., Li, J., Li, Z., Liang, Y., Lin, X., Liu, X., Mattei, B., McIntosh, T.C., McLeod, M.P., McPherson, D., Merkulov, G., Milshina, N.V., Mobarry, C., Morris, J., Moshrefi, A., Mount, S.M., Moy, M., Murphy, B., Murphy, L., Muzny, D.M., Nelson, D.L., Nelson, D.R., Nelson, K.A., Nixon, K., Nusskern, D.R., Pacleb, J.M., Palazzolo, M., Pittman, G.S., Pan, S., Pollard, J., Puri, V., Reese, M.G., Reinert, K., Remington, K., Saunders, R.D., Scheeler, F., Shen, H., Shue, B.C., Siden-Kiamos, I., Simpson, M., Skupski, M.P., Smith, T., Spier, E., Spradling, A.C., Stapleton, M., Strong, R., Sun, E., Svirskas, R., Tector, C., Turner, R., Venter, E., Wang, A.H., Wang, X., Wang, Z.Y., Wassarman, D.A., Weinstock, G.M., Weissenbach, J., Williams, S.M., WoodageT, Worley, K.C., Wu, D., Yang, S., Yao, Q.A., Ye, J., Yeh, R.F., Zaveri, J.S., Zhan, M., Zhang, G., Zhao, Q., Zheng, L., Zheng, X.H., Zhong, F.N., Zhong, W., Zhou, X., Zhu, S., Zhu, X., Smith, H.O., Gibbs, R.A., Myers, E.W., Rubin, G.M., and Venter, J.C. (2000). The genome sequence of Drosophila melanogaster. Science **287,** 2185-2195.

Amborella Genome, P. (2013). The Amborella genome and the evolution of flowering plants. Science **342,** 1241089.

Atkins, K.C., and Cross, F.R. (2018). Interregulation of CDKA/CDK1 and the Plant-Specific Cyclin-Dependent Kinase CDKB in Control of the Chlamydomonas Cell Cycle. Plant Cell **30,** 429-446.

Attrill, S.T., Mulvey, H., Champion, C., and Dolan, L. (2024). Microtubules and actin filaments direct nuclear movement during the polarisation of Marchantia spore cells. Development **151**.

Azumi, Y., Liu, D., Zhao, D., Li, W., Wang, G., Hu, Y., and Ma, H. (2002). Homolog interaction during meiotic prophase I in Arabidopsis requires the SOLO DANCERS gene encoding a novel cyclin-like protein. EMBO J **21,** 3081-3095.

Bainard, J.D., Forrest, L.L., Goffinet, B., and Newmaster, S.G. (2013). Nuclear DNA content variation and evolution in liverworts. Mol Phylogenet Evol **68,** 619-627.

Bao, L., Inoue, N., Ishikawa, M., Gotoh, E., Teh, O.K., Higa, T., Morimoto, T., Ginanjar, E.F., Harashima, H., Noda, N., Watahiki, M., Hiwatashi, Y., Sekine, M., Hasebe, M., Wada, M., and Fujita, T. (2022). A PSTAIRE-type cyclin-dependent kinase controls light responses in land plants. Sci Adv **8,** eabk2116.

Bi, G., Zhao, S., Yao, J., Wang, H., Zhao, M., Sun, Y., Hou, X., Haas, F.B., Varshney, D., Prigge, M., Rensing, S.A., Jiao, Y., Ma, Y., Yan, J., and Dai, J. (2024). Near telomere-to-telomere genome of the model plant Physcomitrium patens. Nat Plants **10,** 327-343.

Boruc, J., Mylle, E., Duda, M., De Clercq, R., Rombauts, S., Geelen, D., Hilson, P., Inze, D., Van Damme, D., and Russinova, E. (2010). Systematic localization of the Arabidopsis core cell cycle proteins reveals novel cell division complexes. Plant Physiol **152,** 553-565.

Bowler, C., Allen, A.E., Badger, J.H., Grimwood, J., Jabbari, K., Kuo, A., Maheswari, U., Martens, C., Maumus, F., Otillar, R.P., Rayko, E., Salamov, A., Vandepoele, K., Beszteri, B., Gruber, A., Heijde, M., Katinka, M., Mock, T., Valentin, K., Verret, F., Berges, J.A., Brownlee, C., Cadoret, J.P., Chiovitti, A., Choi, C.J., Coesel, S., De Martino, A., Detter, J.C., Durkin, C., Falciatore, A., Fournet, J., Haruta, M., Huysman, M.J., Jenkins, B.D., Jiroutova, K., Jorgensen, R.E., Joubert, Y., Kaplan, A., Kroger, N., Kroth, P.G., La Roche, J., Lindquist, E., Lommer, M., Martin-Jezequel, V., Lopez, P.J., Lucas, S., Mangogna, M., McGinnis, K., Medlin, L.K., Montsant, A., Oudot-Le Secq, M.P., Napoli, C., Obornik, M., Parker, M.S., Petit, J.L., Porcel, B.M., Poulsen, N., Robison, M., Rychlewski, L., Rynearson, T.A., Schmutz, J., Shapiro, H., Siaut, M., Stanley, M., Sussman, M.R., Taylor, A.R., Vardi, A., von Dassow, P., Vyverman, W., Willis, A., Wyrwicz, L.S., Rokhsar, D.S., Weissenbach, J., Armbrust, E.V., Green, B.R., Van de Peer, Y., and Grigoriev, I.V. (2008). The Phaeodactylum genome reveals the evolutionary history of diatom genomes. Nature **456,** 239-244.

Bowman, J.L., Arteaga-Vazquez, M., Berger, F., Briginshaw, L.N., Carella, P., Aguilar-Cruz, A., Davies, K.M., Dierschke, T., Dolan, L., Dorantes-Acosta, A.E., Fisher, T.J., Flores-Sandoval, E., Futagami, K., Ishizaki, K., Jibran, R., Kanazawa, T., Kato, H., Kohchi, T., Levins, J., Lin, S.S., Nakagami, H., Nishihama, R., Romani, F., Schornack, S., Tanizawa, Y., Tsuzuki, M., Ueda, T., Watanabe, Y., Yamato, K.T., and Zachgo, S. (2022). The renaissance and enlightenment of Marchantia as a model system. Plant Cell **34,** 3512-3542.

Bowman, J.L., Kohchi, T., Yamato, K.T., Jenkins, J., Shu, S., Ishizaki, K., Yamaoka, S., Nishihama, R., Nakamura, Y., Berger, F., Adam, C., Aki, S.S., Althoff, F., Araki, T., Arteaga-Vazquez, M.A., Balasubrmanian, S., Barry, K., Bauer, D., Boehm, C.R., Briginshaw, L., Caballero-Perez, J., Catarino, B., Chen, F., Chiyoda, S., Chovatia, M., Davies, K.M., Delmans, M., Demura, T., Dierschke, T., Dolan, L., Dorantes-Acosta, A.E., Eklund, D.M., Florent, S.N., Flores-Sandoval, E., Fujiyama, A., Fukuzawa, H., Galik, B., Grimanelli, D., Grimwood, J., Grossniklaus, U., Hamada, T., Haseloff, J., Hetherington, A.J., Higo, A., Hirakawa, Y., Hundley, H.N., Ikeda, Y., Inoue, K., Inoue, S.I., Ishida, S., Jia, Q., Kakita, M., Kanazawa, T., Kawai, Y., Kawashima, T., Kennedy, M., Kinose, K., Kinoshita, T., Kohara, Y., Koide, E., Komatsu, K., Kopischke, S., Kubo, M., Kyozuka, J., Lagercrantz, U., Lin, S.S., Lindquist, E., Lipzen, A.M., Lu, C.W., De Luna, E., Martienssen, R.A., Minamino, N., Mizutani, M., Mizutani, M., Mochizuki, N., Monte, I., Mosher, R., Nagasaki, H., Nakagami, H., Naramoto, S., Nishitani, K., Ohtani, M., Okamoto, T., Okumura, M., Phillips, J., Pollak, B., Reinders, A., Rovekamp, M., Sano, R., Sawa, S., Schmid, M.W., Shirakawa, M., Solano, R., Spunde, A., Suetsugu, N., Sugano, S., Sugiyama, A., Sun, R., Suzuki, Y., Takenaka, M., Takezawa, D., Tomogane, H., Tsuzuki, M., Ueda, T., Umeda, M., Ward, J.M., Watanabe, Y., Yazaki, K., Yokoyama, R., Yoshitake, Y., Yotsui, I., Zachgo, S., and Schmutz, J. (2017). Insights into Land Plant Evolution Garnered from the Marchantia polymorpha Genome. Cell **171,** 287-304 e215.

Breker, M., Lieberman, K., and Cross, F.R. (2018). Comprehensive Discovery of Cell-Cycle-Essential Pathways in Chlamydomonas reinhardtii. Plant Cell **30,** 1178-1198.

845 **Brophy, J.A.N., LaRue, T., and Dinneny, J.R.** (2018). Understanding and engineering
846 plant form. Semin Cell Dev Biol **79,** 68-77.
847 **Charif, D., and Lobry, J.R.** (2007). SeqinR 1.0-2: A Contributed Package to the R Project
848 for Statistical Computing Devoted to Biological Sequences Retrieval and
849 Analysis. In Structural Approaches to Sequence Evolution: Molecules, Networks,
850 Populations, U. Bastolla, M. Porto, H.E. Roman, and M. Vendruscolo, eds (Berlin,
851 Heidelberg: Springer Berlin Heidelberg), pp. 207-232.
852 **Cheng, S., Xian, W., Fu, Y., Marin, B., Keller, J., Wu, T., Sun, W., Li, X., Xu, Y., Zhang,**
853 **Y., Wittek, S., Reder, T., Gunther, G., Gontcharov, A., Wang, S., Li, L., Liu, X.,**
854 **Wang, J., Yang, H., Xu, X., Delaux, P.M., Melkonian, B., Wong, G.K., and**
855 **Melkonian, M.** (2019). Genomes of Subaerial Zygnematophyceae Provide
856 Insights into Land Plant Evolution. Cell **179,** 1057-1067 e1014.
857 **Clute, P., and Pines, J.** (1999). Temporal and spatial control of cyclin B1 destruction in
858 metaphase. Nat Cell Biol **1,** 82-87.
859 **Cock, J.M., Sterck, L., Rouze, P., Scornet, D., Allen, A.E., Amoutzias, G., Anthouard,**
860 **V., Artiguenave, F., Aury, J.M., Badger, J.H., Beszteri, B., Billiau, K., Bonnet, E.,**
861 **Bothwell, J.H., Bowler, C., Boyen, C., Brownlee, C., Carrano, C.J., Charrier, B.,**
862 **Cho, G.Y., Coelho, S.M., Collen, J., Corre, E., Da Silva, C., Delage, L.,**
863 **Delaroque, N., Dittami, S.M., Doulbeau, S., Elias, M., Farnham, G., Gachon,**
864 **C.M., Gschloessl, B., Heesch, S., Jabbari, K., Jubin, C., Kawai, H., Kimura, K.,**
865 **Kloareg, B., Kupper, F.C., Lang, D., Le Bail, A., Leblanc, C., Lerouge, P., Lohr,**
866 **M., Lopez, P.J., Martens, C., Maumus, F., Michel, G., Miranda-Saavedra, D.,**
867 **Morales, J., Moreau, H., Motomura, T., Nagasato, C., Napoli, C.A., Nelson,**
868 **D.R., Nyvall-Collen, P., Peters, A.F., Pommier, C., Potin, P., Poulain, J.,**
869 **Quesneville, H., Read, B., Rensing, S.A., Ritter, A., Rousvoal, S., Samanta, M.,**
870 **Samson, G., Schroeder, D.C., Segurens, B., Strittmatter, M., Tonon, T.,**
871 **Tregear, J.W., Valentin, K., von Dassow, P., Yamagishi, T., Van de Peer, Y., and**
872 **Wincker, P.** (2010). The Ectocarpus genome and the independent evolution of
873 multicellularity in brown algae. Nature **465,** 617-621.
874 **Consortium, C.e.S.** (1998). Genome sequence of the nematode C. elegans: a platform
875 for investigating biology. Science **282,** 2012-2018.
876 **Cross, F.R.** (2020). Regulation of Multiple Fission and Cell-Cycle-Dependent Gene
877 Expression by CDKA1 and the Rb-E2F Pathway in Chlamydomonas. Curr Biol **30,**
878 1855-1865 e1854.
879 **Cross, F.R., and Umen, J.G.** (2015). The Chlamydomonas cell cycle. Plant J **82,** 370-392.
880 **d'Erfurth, I., Cromer, L., Jolivet, S., Girard, C., Horlow, C., Sun, Y., To, J.P.,**
881 **Berchowitz, L.E., Copenhaver, G.P., and Mercier, R.** (2010). The cyclin-A
882 CYCA1;2/TAM is required for the meiosis I to meiosis II transition and cooperates
883 with OSD1 for the prophase to first meiotic division transition. PLoS Genet **6,**
884 e1000989.
885 **Datar, S.A., Jacobs, H.W., de la Cruz, A.F., Lehner, C.F., and Edgar, B.A.** (2000). The
886 Drosophila cyclin D-Cdk4 complex promotes cellular growth. EMBO J **19,** 4543-
887 4554.
888 **Dewitte, W., Riou-Khamlichi, C., Scofield, S., Healy, J.M., Jacqmard, A., Kilby, N.J.,**
889 **and Murray, J.A.** (2003). Altered cell cycle distribution, hyperplasia, and inhibited
890 differentiation in Arabidopsis caused by the D-type cyclin CYCD3. Plant Cell **15,**
891 79-92.

Doerner, P., Jorgensen, J.E., You, R., Steppuhn, J., and Lamb, C. (1996). Control of root growth and development by cyclin expression. Nature **380,** 520-523.

Doonan, J., and Hunt, T. (1996). Cell cycle. Why don't plants get cancer? Nature **380,** 481-482.

Feng, G., Burleigh, J.G., Braun, E.L., Mei, W., and Barbazuk, W.B. (2017). Evolution of the 3R-MYB Gene Family in Plants. Genome Biol Evol **9,** 1013-1029.

Feng, X., Zheng, J., Irisarri, I., Yu, H., Zheng, B., Ali, Z., de Vries, S., Keller, J., Furst-Jansen, J.M.R., Dadras, A., Zegers, J.M.S., Rieseberg, T.P., Dhabalia Ashok, A., Darienko, T., Bierenbroodspot, M.J., Gramzow, L., Petroll, R., Haas, F.B., Fernandez-Pozo, N., Nousias, O., Li, T., Fitzek, E., Grayburn, W.S., Rittmeier, N., Permann, C., Rumpler, F., Archibald, J.M., Theissen, G., Mower, J.P., Lorenz, M., Buschmann, H., von Schwartzenberg, K., Boston, L., Hayes, R.D., Daum, C., Barry, K., Grigoriev, I.V., Wang, X., Li, F.W., Rensing, S.A., Ben Ari, J., Keren, N., Mosquna, A., Holzinger, A., Delaux, P.M., Zhang, C., Huang, J., Mutwil, M., de Vries, J., and Yin, Y. (2024). Genomes of multicellular algal sisters to land plants illuminate signaling network evolution. Nat Genet **56,** 1018-1031.

Finn, R.D., Clements, J., and Eddy, S.R. (2011). HMMER web server: interactive sequence similarity searching. Nucleic Acids Res **39,** W29-37.

Geley, S., Kramer, E., Gieffers, C., Gannon, J., Peters, J.M., and Hunt, T. (2001). Anaphase-promoting complex/cyclosome-dependent proteolysis of human cyclin A starts at the beginning of mitosis and is not subject to the spindle assembly checkpoint. J Cell Biol **153,** 137-148.

Goffeau, A., Barrell, B.G., Bussey, H., Davis, R.W., Dujon, B., Feldmann, H., Galibert, F., Hoheisel, J.D., Jacq, C., Johnston, M., Louis, E.J., Mewes, H.W., Murakami, Y., Philippsen, P., Tettelin, H., and Oliver, S.G. (1996). Life with 6000 genes. Science **274,** 546, 563-547.

Gutierrez, C. (2009). The Arabidopsis cell division cycle. Arabidopsis Book **7,** e0120.

Gutierrez, C. (2022). A Journey to the Core of the Plant Cell Cycle. Int J Mol Sci **23**.

Hao, Y., Stuart, T., Kowalski, M.H., Choudhary, S., Hoffman, P., Hartman, A., Srivastava, A., Molla, G., Madad, S., Fernandez-Granda, C., and Satija, R. (2024). Dictionary learning for integrative, multimodal and scalable single-cell analysis. Nat Biotechnol **42,** 293-304.

Hori, K., Maruyama, F., Fujisawa, T., Togashi, T., Yamamoto, N., Seo, M., Sato, S., Yamada, T., Mori, H., Tajima, N., Moriyama, T., Ikeuchi, M., Watanabe, M., Wada, H., Kobayashi, K., Saito, M., Masuda, T., Sasaki-Sekimoto, Y., Mashiguchi, K., Awai, K., Shimojima, M., Masuda, S., Iwai, M., Nobusawa, T., Narise, T., Kondo, S., Saito, H., Sato, R., Murakawa, M., Ihara, Y., Oshima-Yamada, Y., Ohtaka, K., Satoh, M., Sonobe, K., Ishii, M., Ohtani, R., Kanamori-Sato, M., Honoki, R., Miyazaki, D., Mochizuki, H., Umetsu, J., Higashi, K., Shibata, D., Kamiya, Y., Sato, N., Nakamura, Y., Tabata, S., Ida, S., Kurokawa, K., and Ohta, H. (2014). Klebsormidium flaccidum genome reveals primary factors for plant terrestrial adaptation. Nat Commun **5,** 3978.

Imai, K.K., Ohashi, Y., Tsuge, T., Yoshizumi, T., Matsui, M., Oka, A., and Aoyama, T. (2006). The A-type cyclin CYCA2;3 is a key regulator of ploidy levels in Arabidopsis endoreduplication. Plant Cell **18,** 382-396.

Inze, D., and De Veylder, L. (2006). Cell cycle regulation in plant development. Annu Rev Genet **40,** 77-105.

Ishida, S., Suzuki, H., Iwaki, A., Kawamura, S., Yamaoka, S., Kojima, M., Takebayashi, Y., Yamaguchi, K., Shigenobu, S., Sakakibara, H., Kohchi, T., and Nishihama, R. (2022). Diminished Auxin Signaling Triggers Cellular Reprogramming by Inducing a Regeneration Factor in the Liverwort Marchantia polymorpha. Plant Cell Physiol **63,** 384-400.

Ishikawa, M., Murata, T., Sato, Y., Nishiyama, T., Hiwatashi, Y., Imai, A., Kimura, M., Sugimoto, N., Akita, A., Oguri, Y., Friedman, W.E., Hasebe, M., and Kubo, M. (2011). Physcomitrella cyclin-dependent kinase A links cell cycle reactivation to other cellular changes during reprogramming of leaf cells. Plant Cell **23,** 2924-2938.

Ito, M., Araki, S., Matsunaga, S., Itoh, T., Nishihama, R., Machida, Y., Doonan, J.H., and Watanabe, A. (2001). G2/M-phase-specific transcription during the plant cell cycle is mediated by c-Myb-like transcription factors. Plant Cell **13,** 1891-1905.

Jiao, C., Sorensen, I., Sun, X., Sun, H., Behar, H., Alseekh, S., Philippe, G., Palacio Lopez, K., Sun, L., Reed, R., Jeon, S., Kiyonami, R., Zhang, S., Fernie, A.R., Brumer, H., Domozych, D.S., Fei, Z., and Rose, J.K.C. (2020). The Penium margaritaceum Genome: Hallmarks of the Origins of Land Plants. Cell **181,** 1097-1111 e1012.

Joubes, J., Chevalier, C., Dudits, D., Heberle-Bors, E., Inze, D., Umeda, M., and Renaudin, J.P. (2000). CDK-related protein kinases in plants. Plant Mol Biol **43,** 607-620.

Katoh, K., Misawa, K., Kuma, K., and Miyata, T. (2002). MAFFT: a novel method for rapid multiple sequence alignment based on fast Fourier transform. Nucleic Acids Res **30,** 3059-3066.

Kawamura, S., Romani, F., Yagura, M., Mochizuki, T., Sakamoto, M., Yamaoka, S., Nishihama, R., Nakamura, Y., Yamato, K.T., Bowman, J.L., Kohchi, T., and Tanizawa, Y. (2022). MarpolBase Expression: A Web-Based, Comprehensive Platform for Visualization and Analysis of Transcriptomes in the Liverwort Marchantia polymorpha. Plant Cell Physiol **63,** 1745-1755.

Kobayashi, K., Suzuki, T., Iwata, E., Magyar, Z., Bogre, L., and Ito, M. (2015). MYB3Rs, plant homologs of Myb oncoproteins, control cell cycle-regulated transcription and form DREAM-like complexes. Transcription **6,** 106-111.

Komaki, S., and Sugimoto, K. (2012). Control of the plant cell cycle by developmental and environmental cues. Plant Cell Physiol **53,** 953-964.

Koroleva, O.A., Tomlinson, M., Parinyapong, P., Sakvarelidze, L., Leader, D., Shaw, P., and Doonan, J.H. (2004). CycD1, a putative G1 cyclin from Antirrhinum majus, accelerates the cell cycle in cultured tobacco BY-2 cells by enhancing both G1/S entry and progression through S and G2 phases. Plant Cell **16,** 2364-2379.

Krylov, D.M., Nasmyth, K., and Koonin, E.V. (2003). Evolution of eukaryotic cell cycle regulation: stepwise addition of regulatory kinases and late advent of the CDKs. Curr Biol **13,** 173-177.

Letunic, I., and Bork, P. (2024). Interactive Tree of Life (iTOL) v6: recent updates to the phylogenetic tree display and annotation tool. Nucleic Acids Res **52,** W78-W82.

Li, F.W., Nishiyama, T., Waller, M., Frangedakis, E., Keller, J., Li, Z., Fernandez-Pozo, N., Barker, M.S., Bennett, T., Blazquez, M.A., Cheng, S., Cuming, A.C., de Vries, J., de Vries, S., Delaux, P.M., Diop, I.S., Harrison, C.J., Hauser, D., Hernandez-Garcia, J., Kirbis, A., Meeks, J.C., Monte, I., Mutte, S.K., Neubauer,

986 **A., Quandt, D., Robison, T., Shimamura, M., Rensing, S.A., Villarreal, J.C.,**
987 **Weijers, D., Wicke, S., Wong, G.K., Sakakibara, K., and Szovenyi, P.** (2020a).
988 Anthoceros genomes illuminate the origin of land plants and the unique biology
989 of hornworts. Nat Plants **6,** 259-272.
990 **Li, L., Wang, S., Wang, H., Sahu, S.K., Marin, B., Li, H., Xu, Y., Liang, H., Li, Z., Cheng,**
991 **S., Reder, T., Cebi, Z., Wittek, S., Petersen, M., Melkonian, B., Du, H., Yang, H.,**
992 **Wang, J., Wong, G.K., Xu, X., Liu, X., Van de Peer, Y., Melkonian, M., and Liu,**
993 **H.** (2020b). The genome of Prasinoderma coloniale unveils the existence of a third
994 phylum within green plants. Nat Ecol Evol **4,** 1220-1231.
995 **Liang, Z., Geng, Y., Ji, C., Du, H., Wong, C.E., Zhang, Q., Zhang, Y., Zhang, P., Riaz, A.,**
996 **Chachar, S., Ding, Y., Wen, J., Wu, Y., Wang, M., Zheng, H., Wu, Y., Demko, V.,**
997 **Shen, L., Han, X., Zhang, P., Gu, X., and Yu, H.** (2020). Mesostigma viride
998 Genome and Transcriptome Provide Insights into the Origin and Evolution of
999 Streptophyta. Adv Sci (Weinh) **7,** 1901850.
1000 **Lifschitz, S., Haeusler, E.H., Catanho, M., Miranda, A.B., Armas, E.M., Heine, A.,**
1001 **Moreira, S., and Tristao, C.** (2022). Bio-Strings: A Relational Database Data-Type
1002 for Dealing with Large Biosequences. BioTech (Basel) **11**.
1003 **Linde, A.M., Sawangproh, W., Cronberg, N., Szovenyi, P., and Lagercrantz, U.** (2020).
1004 Evolutionary History of the Marchantia polymorpha Complex. Front Plant Sci **11,**
1005 829.
1006 **Liu, J., and Kipreos, E.T.** (2000). Evolution of cyclin-dependent kinases (CDKs) and CDK-
1007 activating kinases (CAKs): differential conservation of CAKs in yeast and metazoa.
1008 Mol Biol Evol **17,** 1061-1074.
1009 **Liu, W., Cai, G., Zhai, N., Wang, H., Tang, T., Zhang, Y., Zhang, Z., Sun, L., Zhang, Y.,**
1010 **Beeckman, T., and Xu, L.** (2023). Genome and transcriptome of Selaginella
1011 kraussiana reveal evolution of root apical meristems in vascular plants. Curr Biol
1012 **33,** 4085-4097 e4085.
1013 **Ma, Z., Wu, Y., Jin, J., Yan, J., Kuang, S., Zhou, M., Zhang, Y., and Guo, A.Y.** (2013).
1014 Phylogenetic analysis reveals the evolution and diversification of cyclins in
1015 eukaryotes. Mol Phylogenet Evol **66,** 1002-1010.
1016 **Marchant, D.B., Chen, G., Cai, S., Chen, F., Schafran, P., Jenkins, J., Shu, S., Plott,**
1017 **C., Webber, J., Lovell, J.T., He, G., Sandor, L., Williams, M., Rajasekar, S.,**
1018 **Healey, A., Barry, K., Zhang, Y., Sessa, E., Dhakal, R.R., Wolf, P.G., Harkess,**
1019 **A., Li, F.W., Rossner, C., Becker, A., Gramzow, L., Xue, D., Wu, Y., Tong, T.,**
1020 **Wang, Y., Dai, F., Hua, S., Wang, H., Xu, S., Xu, F., Duan, H., Theissen, G.,**
1021 **McKain, M.R., Li, Z., McKibben, M.T.W., Barker, M.S., Schmitz, R.J.,**
1022 **Stevenson, D.W., Zumajo-Cardona, C., Ambrose, B.A., Leebens-Mack, J.H.,**
1023 **Grimwood, J., Schmutz, J., Soltis, P.S., Soltis, D.E., and Chen, Z.H.** (2022).
1024 Dynamic genome evolution in a model fern. Nat Plants **8,** 1038-1051.
1025 **Martinez-Alonso, D., and Malumbres, M.** (2020). Mammalian cell cycle cyclins. Semin
1026 Cell Dev Biol **107,** 28-35.
1027 **Matsuzaki, M., Misumi, O., Shin, I.T., Maruyama, S., Takahara, M., Miyagishima, S.Y.,**
1028 **Mori, T., Nishida, K., Yagisawa, F., Nishida, K., Yoshida, Y., Nishimura, Y.,**
1029 **Nakao, S., Kobayashi, T., Momoyama, Y., Higashiyama, T., Minoda, A., Sano,**
1030 **M., Nomoto, H., Oishi, K., Hayashi, H., Ohta, F., Nishizaka, S., Haga, S., Miura,**
1031 **S., Morishita, T., Kabeya, Y., Terasawa, K., Suzuki, Y., Ishii, Y., Asakawa, S.,**
1032 **Takano, H., Ohta, N., Kuroiwa, H., Tanaka, K., Shimizu, N., Sugano, S., Sato,**

1033 **N., Nozaki, H., Ogasawara, N., Kohara, Y., and Kuroiwa, T.** (2004). Genome
1034 sequence of the ultrasmall unicellular red alga Cyanidioschyzon merolae 10D.
1035 Nature **428,** 653-657.
1036 **Menges, M., de Jager, S.M., Gruissem, W., and Murray, J.A.** (2005). Global analysis of
1037 the core cell cycle regulators of Arabidopsis identifies novel genes, reveals
1038 multiple and highly specific profiles of expression and provides a coherent model
1039 for plant cell cycle control. Plant J **41,** 546-566.
1040 **Menges, M., Samland, A.K., Planchais, S., and Murray, J.A.** (2006). The D-type cyclin
1041 CYCD3;1 is limiting for the G1-to-S-phase transition in Arabidopsis. Plant Cell **18,**
1042 893-906.
1043 **Merchant, S.S., Prochnik, S.E., Vallon, O., Harris, E.H., Karpowicz, S.J., Witman,**
1044 **G.B., Terry, A., Salamov, A., Fritz-Laylin, L.K., Marechal-Drouard, L., Marshall,**
1045 **W.F., Qu, L.H., Nelson, D.R., Sanderfoot, A.A., Spalding, M.H., Kapitonov,**
1046 **V.V., Ren, Q., Ferris, P., Lindquist, E., Shapiro, H., Lucas, S.M., Grimwood, J.,**
1047 **Schmutz, J., Cardol, P., Cerutti, H., Chanfreau, G., Chen, C.L., Cognat, V.,**
1048 **Croft, M.T., Dent, R., Dutcher, S., Fernandez, E., Fukuzawa, H., Gonzalez-**
1049 **Ballester, D., Gonzalez-Halphen, D., Hallmann, A., Hanikenne, M., Hippler,**
1050 **M., Inwood, W., Jabbari, K., Kalanon, M., Kuras, R., Lefebvre, P.A., Lemaire,**
1051 **S.D., Lobanov, A.V., Lohr, M., Manuell, A., Meier, I., Mets, L., Mittag, M.,**
1052 **Mittelmeier, T., Moroney, J.V., Moseley, J., Napoli, C., Nedelcu, A.M., Niyogi,**
1053 **K., Novoselov, S.V., Paulsen, I.T., Pazour, G., Purton, S., Ral, J.P., Riano-**
1054 **Pachon, D.M., Riekhof, W., Rymarquis, L., Schroda, M., Stern, D., Umen, J.,**
1055 **Willows, R., Wilson, N., Zimmer, S.L., Allmer, J., Balk, J., Bisova, K., Chen, C.J.,**
1056 **Elias, M., Gendler, K., Hauser, C., Lamb, M.R., Ledford, H., Long, J.C.,**
1057 **Minagawa, J., Page, M.D., Pan, J., Pootakham, W., Roje, S., Rose, A.,**
1058 **Stahlberg, E., Terauchi, A.M., Yang, P., Ball, S., Bowler, C., Dieckmann, C.L.,**
1059 **Gladyshev, V.N., Green, P., Jorgensen, R., Mayfield, S., Mueller-Roeber, B.,**
1060 **Rajamani, S., Sayre, R.T., Brokstein, P., Dubchak, I., Goodstein, D., Hornick,**
1061 **L., Huang, Y.W., Jhaveri, J., Luo, Y., Martinez, D., Ngau, W.C., Otillar, B.,**
1062 **Poliakov, A., Porter, A., Szajkowski, L., Werner, G., Zhou, K., Grigoriev, I.V.,**
1063 **Rokhsar, D.S., and Grossman, A.R.** (2007). The Chlamydomonas genome
1064 reveals the evolution of key animal and plant functions. Science **318,** 245-250.
1065 **Minh, B.Q., Schmidt, H.A., Chernomor, O., Schrempf, D., Woodhams, M.D., von**
1066 **Haeseler, A., and Lanfear, R.** (2020). IQ-TREE 2: New Models and Efficient
1067 Methods for Phylogenetic Inference in the Genomic Era. Mol Biol Evol **37,** 1530-
1068 1534.
1069 **Mironov, V.V., De Veylder, L., Van Montagu, M., and Inze, D.** (1999). Cyclin-dependent
1070 kinases and cell division in plants- the nexus. Plant Cell **11,** 509-522.
1071 **Montgomery, S.A., Tanizawa, Y., Galik, B., Wang, N., Ito, T., Mochizuki, T.,**
1072 **Akimcheva, S., Bowman, J.L., Cognat, V., Marechal-Drouard, L., Ekker, H.,**
1073 **Hong, S.F., Kohchi, T., Lin, S.S., Liu, L.D., Nakamura, Y., Valeeva, L.R.,**
1074 **Shakirov, E.V., Shippen, D.E., Wei, W.L., Yagura, M., Yamaoka, S., Yamato,**
1075 **K.T., Liu, C., and Berger, F.** (2020). Chromatin Organization in Early Land Plants
1076 Reveals an Ancestral Association between H3K27me3, Transposons, and
1077 Constitutive Heterochromatin. Curr Biol **30,** 573-588 e577.
1078 **Nagai, I.** (1919). Induced Adventitious Growth in the Gemnnae of Marchanti. The
1079 Botanical Magazine **33,** 99-109.

Nishihama, R., Ishida, S., Urawa, H., Kamei, Y., and Kohchi, T. (2016). Conditional Gene Expression/Deletion Systems for Marchantia polymorpha Using its Own Heat-Shock Promoter and Cre/loxP-Mediated Site-Specific Recombination. Plant Cell Physiol **57,** 271-280.

Nishihama, R., Ishizaki, K., Hosaka, M., Matsuda, Y., Kubota, A., and Kohchi, T. (2015). Phytochrome-mediated regulation of cell division and growth during regeneration and sporeling development in the liverwort Marchantia polymorpha. J Plant Res **128,** 407-421.

Nishiyama, T., Sakayama, H., de Vries, J., Buschmann, H., Saint-Marcoux, D., Ullrich, K.K., Haas, F.B., Vanderstraeten, L., Becker, D., Lang, D., Vosolsobe, S., Rombauts, S., Wilhelmsson, P.K.I., Janitza, P., Kern, R., Heyl, A., Rumpler, F., Villalobos, L., Clay, J.M., Skokan, R., Toyoda, A., Suzuki, Y., Kagoshima, H., Schijlen, E., Tajeshwar, N., Catarino, B., Hetherington, A.J., Saltykova, A., Bonnot, C., Breuninger, H., Symeonidi, A., Radhakrishnan, G.V., Van Nieuwerburgh, F., Deforce, D., Chang, C., Karol, K.G., Hedrich, R., Ulvskov, P., Glockner, G., Delwiche, C.F., Petrasek, J., Van de Peer, Y., Friml, J., Beilby, M., Dolan, L., Kohara, Y., Sugano, S., Fujiyama, A., Delaux, P.M., Quint, M., Theissen, G., Hagemann, M., Harholt, J., Dunand, C., Zachgo, S., Langdale, J., Maumus, F., Van Der Straeten, D., Gould, S.B., and Rensing, S.A. (2018). The Chara Genome: Secondary Complexity and Implications for Plant Terrestrialization. Cell **174,** 448-464 e424.

Nowack, M.K., Harashima, H., Dissmeyer, N., Zhao, X., Bouyer, D., Weimer, A.K., De Winter, F., Yang, F., and Schnittger, A. (2012). Genetic framework of cyclin-dependent kinase function in Arabidopsis. Dev Cell **22,** 1030-1040.

Palenik, B., Grimwood, J., Aerts, A., Rouze, P., Salamov, A., Putnam, N., Dupont, C., Jorgensen, R., Derelle, E., Rombauts, S., Zhou, K., Otillar, R., Merchant, S.S., Podell, S., Gaasterland, T., Napoli, C., Gendler, K., Manuell, A., Tai, V., Vallon, O., Piganeau, G., Jancek, S., Heijde, M., Jabbari, K., Bowler, C., Lohr, M., Robbens, S., Werner, G., Dubchak, I., Pazour, G.J., Ren, Q., Paulsen, I., Delwiche, C., Schmutz, J., Rokhsar, D., Van de Peer, Y., Moreau, H., and Grigoriev, I.V. (2007). The tiny eukaryote Ostreococcus provides genomic insights into the paradox of plankton speciation. Proc Natl Acad Sci U S A **104,** 7705-7710.

Patron, N.J., Orzaez, D., Marillonnet, S., Warzecha, H., Matthewman, C., Youles, M., Raitskin, O., Leveau, A., Farre, G., Rogers, C., Smith, A., Hibberd, J., Webb, A.A., Locke, J., Schornack, S., Ajioka, J., Baulcombe, D.C., Zipfel, C., Kamoun, S., Jones, J.D., Kuhn, H., Robatzek, S., Van Esse, H.P., Sanders, D., Oldroyd, G., Martin, C., Field, R., O'Connor, S., Fox, S., Wulff, B., Miller, B., Breakspear, A., Radhakrishnan, G., Delaux, P.M., Loque, D., Granell, A., Tissier, A., Shih, P., Brutnell, T.P., Quick, W.P., Rischer, H., Fraser, P.D., Aharoni, A., Raines, C., South, P.F., Ane, J.M., Hamberger, B.R., Langdale, J., Stougaard, J., Bouwmeester, H., Udvardi, M., Murray, J.A., Ntoukakis, V., Schafer, P., Denby, K., Edwards, K.J., Osbourn, A., and Haseloff, J. (2015). Standards for plant synthetic biology: a common syntax for exchange of DNA parts. New Phytol **208,** 13-19.

1125 **Pecani, K., Lieberman, K., Tajima-Shirasaki, N., Onishi, M., and Cross, F.R.** (2022).
1126 Control of division in Chlamydomonas by cyclin B/CDKB1 and the anaphase-
1127 promoting complex. PLoS Genet **18,** e1009997.
1128 **Peramuna, A., Lopez, C.Q., Rios, F.J.A., Bae, H., Fangel, J.U., Batth, R., Harholt, J.,**
1129 **and Simonsen, H.T.** (2023). Overexpression of Physcomitrium patens cell cycle
1130 regulators leads to larger gametophytes. Sci Rep **13,** 4301.
1131 **Procter, J.B., Carstairs, G.M., Soares, B., Mourao, K., Ofoegbu, T.C., Barton, D., Lui,**
1132 **L., Menard, A., Sherstnev, N., Roldan-Martinez, D., Duce, S., Martin, D.M.A.,**
1133 **and Barton, G.J.** (2021). Alignment of Biological Sequences with Jalview. Methods
1134 Mol Biol **2231,** 203-224.
1135 **Quevillon, E., Silventoinen, V., Pillai, S., Harte, N., Mulder, N., Apweiler, R., and**
1136 **Lopez, R.** (2005). InterProScan: protein domains identifier. Nucleic Acids Res **33,**
1137 W116-120.
1138 **Radhakrishnan, G.V., Keller, J., Rich, M.K., Vernie, T., Mbadinga Mbadinga, D.L.,**
1139 **Vigneron, N., Cottret, L., Clemente, H.S., Libourel, C., Cheema, J., Linde,**
1140 **A.M., Eklund, D.M., Cheng, S., Wong, G.K.S., Lagercrantz, U., Li, F.W.,**
1141 **Oldroyd, G.E.D., and Delaux, P.M.** (2020). An ancestral signalling pathway is
1142 conserved in intracellular symbioses-forming plant lineages. Nat Plants **6,** 280-
1143 289.
1144 **Rauber, R., Cabreira, C., de Freitas, L.B., Turchetto-Zolet, A.C., and Margis-Pinheiro,**
1145 **M.** (2016). The evolutionary history of the E2F and DEL genes in Viridiplantae. Mol
1146 Phylogenet Evol **99,** 225-234.
1147 **Romani, F., Sauret-Gueto, S., Rebmann, M., Annese, D., Bonter, I., Tomaselli, M.,**
1148 **Dierschke, T., Delmans, M., Frangedakis, E., Silvestri, L., Rever, J., Bowman,**
1149 **J.L., Romani, I., and Haseloff, J.** (2024). The landscape of transcription factor
1150 promoter activity during vegetative development in Marchantia. Plant Cell **36,**
1151 2140-2159.
1152 **Sakamoto, Y., Ishimoto, A., Sakai, Y., Sato, M., Nishihama, R., Abe, K., Sano, Y.,**
1153 **Furuichi, T., Tsuji, H., Kohchi, T., and Matsunaga, S.** (2022). Improved clearing
1154 method contributes to deep imaging of plant organs. Commun Biol **5,** 12.
1155 **Sauret-Gueto, S., Frangedakis, E., Silvestri, L., Rebmann, M., Tomaselli, M., Markel,**
1156 **K., Delmans, M., West, A., Patron, N.J., and Haseloff, J.** (2020). Systematic
1157 Tools for Reprogramming Plant Gene Expression in a Simple Model, Marchantia
1158 polymorpha. ACS Synth Biol **9,** 864-882.
1159 **Schnittger, A., and De Veylder, L.** (2018). The Dual Face of Cyclin B1. Trends Plant Sci
1160 **23,** 475-478.
1161 **Schnittger, A., Schobinger, U., Stierhof, Y.D., and Hulskamp, M.** (2002a). Ectopic B-
1162 type cyclin expression induces mitotic cycles in endoreduplicating Arabidopsis
1163 trichomes. Curr Biol **12,** 415-420.
1164 **Schnittger, A., Schobinger, U., Bouyer, D., Weinl, C., Stierhof, Y.D., and Hulskamp,**
1165 **M.** (2002b). Ectopic D-type cyclin expression induces not only DNA replication but
1166 also cell division in Arabidopsis trichomes. Proc Natl Acad Sci U S A **99,** 6410-
1167 6415.
1168 **Schween, G., Gorr, G., Hohe, A., and Reski, R.** (2008). Unique Tissue-Specific Cell
1169 Cycle in Physcomitrella. Plant Biology **5,** 50-58.
1170 **Siligato, R., Wang, X., Yadav, S.R., Lehesranta, S., Ma, G., Ursache, R., Sevilem, I.,**
1171 **Zhang, J., Gorte, M., Prasad, K., Wrzaczek, M., Heidstra, R., Murphy, A.,**

Scheres, B., and Mahonen, A.P. (2016). MultiSite Gateway-Compatible Cell Type-Specific Gene-Inducible System for Plants. Plant Physiol **170,** 627-641.

Sozzani, R., Maggio, C., Varotto, S., Canova, S., Bergounioux, C., Albani, D., and Cella, R. (2006). Interplay between Arabidopsis activating factors E2Fb and E2Fa in cell cycle progression and development. Plant Physiol **140,** 1355-1366.

Takahashi, I., Kojima, S., Sakaguchi, N., Umeda-Hara, C., and Umeda, M. (2010). Two Arabidopsis cyclin A3s possess G1 cyclin-like features. Plant Cell Rep **29,** 307-315.

Toyoshima, F., Moriguchi, T., Wada, A., Fukuda, M., and Nishida, E. (1998). Nuclear export of cyclin B1 and its possible role in the DNA damage-induced G2 checkpoint. EMBO J **17,** 2728-2735.

Tse, S.W., Annese, D., Romani, F., Guzman-Chavez, F., Bonter, I., Forestier, E., Frangedakis, E., and Haseloff, J. (2024). Optimising promoters and subcellular localisation for constitutive transgene expression in Marchantia polymorpha. Plant Cell Physiol.

Tulin, F., and Cross, F.R. (2014). A microbial avenue to cell cycle control in the plant superkingdom. Plant Cell **26,** 4019-4038.

Tulin, F., and Cross, F.R. (2015). Cyclin-Dependent Kinase Regulation of Diurnal Transcription in Chlamydomonas. Plant Cell **27,** 2727-2742.

Wang, L., Wan, M.C., Liao, R.Y., Xu, J., Xu, Z.G., Xue, H.C., Mai, Y.X., and Wang, J.W. (2023). The maturation and aging trajectory of Marchantia polymorpha at single-cell resolution. Dev Cell.

Wang, W., Haberer, G., Gundlach, H., Glasser, C., Nussbaumer, T., Luo, M.C., Lomsadze, A., Borodovsky, M., Kerstetter, R.A., Shanklin, J., Byrant, D.W., Mockler, T.C., Appenroth, K.J., Grimwood, J., Jenkins, J., Chow, J., Choi, C., Adam, C., Cao, X.H., Fuchs, J., Schubert, I., Rokhsar, D., Schmutz, J., Michael, T.P., Mayer, K.F., and Messing, J. (2014). The Spirodela polyrhiza genome reveals insights into its neotenous reduction fast growth and aquatic lifestyle. Nat Commun **5,** 3311.

Willems, A., Heyman, J., Eekhout, T., Achon, I., Pedroza-Garcia, J.A., Zhu, T., Li, L., Vercauteren, I., Van den Daele, H., van de Cotte, B., De Smet, I., and De Veylder, L. (2020). The Cyclin CYCA3;4 Is a Postprophase Target of the APC/C(CCS52A2) E3-Ligase Controlling Formative Cell Divisions in Arabidopsis. Plant Cell **32,** 2979-2996.

Zhang, T.Q., Chen, Y., and Wang, J.W. (2021). A single-cell analysis of the Arabidopsis vegetative shoot apex. Dev Cell **56,** 1056-1074 e1058.